

Lagged streamflow depletion due to pumping-induced stream drying: Incorporation into analytical streamflow depletion estimation methods

Authors: Sam Zipper^{a,b,*}, Ian Gambill^a, Monty Schmitt^c, Claire Kouba^d, Leland Scantlebury^e, Thomas Harter^f, Nicholas P. Murphy^c

Affiliations:

a. Kansas Geological Survey, University of Kansas, 1930 Constant Ave, Lawrence KS 66044, USA

b. Department of Geology, University of Kansas, 1414 Naismith Drive, Lawrence KS 66045, USA

* Corresponding author: samzipper@ku.edu

c. The Nature Conservancy, 830 S Street, Sacramento CA 95811

d. Yale University, School of the Environment, 195 Prospect Street, New Haven, CT 06511, USA

e. Hydrologic Sciences Graduate Group, University of California, Davis, 1 Shields Ave, Davis CA 95616

f. Department of Land, Air and Water Resources, University of California, Davis, 1 Shields Ave, Davis CA 95616

ORCID + email:

SZ: 0000-0002-8735-5757, samzipper@ku.edu

IG: 0000-0001-7653-4066, ian.gambill@ku.edu

MS: N/A, monty.schmitt@tnc.org

CK: 0000-0002-6381-8315, claire.kouba@yale.edu

LS: 0000-0002-6770-063X, lscantle@ucdavis.edu

TH: 0000-0001-8526-3843, thharter@ucdavis.edu

NM: 0000-0001-8442-0747, nicholas.murphy@tnc.org

Highlights

- Analytical depletion functions (ADFs) estimate streamflow depletion caused by pumping
- Stream drying shifts timing of streamflow depletion due to hydrologic disconnection
- ADFs incorporating stream drying had strong agreement with observed streamflow
- Modeling stream drying requires accurate estimates of non-depleted streamflow
- Strong ADF performance suggests potential use as a low-cost decision-support tool

Revised manuscript submitted to Journal of Hydrology, October 2025.

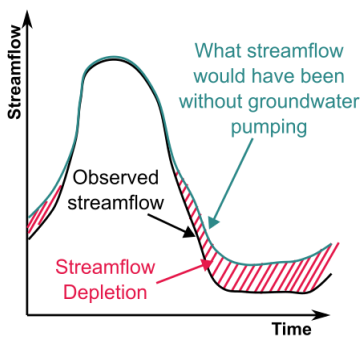
The manuscript has undergone peer review, but is not yet published.

40 **Abstract**

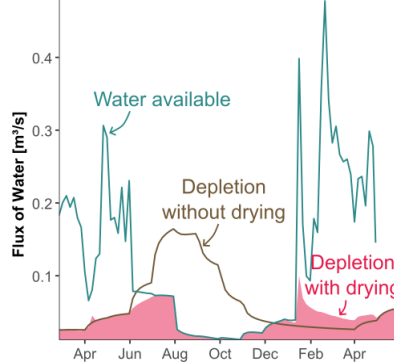
41 Water management often requires accounting for reductions in streamflow caused by
42 groundwater pumping ('streamflow depletion'). Since streamflow depletion cannot be quantified
43 from observational data, it is typically modeled. Analytical depletion functions (ADFs) are a
44 low-cost, low-complexity approach for estimating streamflow depletion with utility for decision
45 support, but ADFs adopt several simplifying assumptions, including an infinite supply of water
46 within the stream. Here, we develop an approach to incorporate stream drying into ADFs to
47 improve their estimation of streamflow and streamflow depletion. Using Scott Valley
48 (California) as an example, we compare ADF results to observed streamflow data and the Scott
49 Valley Integrated Hydrologic Model (SVIHM), a process-based numerical model. ADFs
50 incorporating stream drying have strong agreement with observed streamflow and SVIHM
51 results. Critically, ADFs with drying can simulate a temporal shift in streamflow depletion that
52 occurs when summer stream drying causes stream network disconnections and a substantial
53 fraction of streamflow depletion is lagged until the fall/winter, when the stream network rewets.
54 Estimates of what streamflow would have been without groundwater pumping are required to
55 incorporate stream drying into ADFs, and we evaluate the ability of a statewide statistical model
56 of unimpaired monthly streamflow (the California Natural Flows Database [CNFD]) to meet this
57 need. ADFs using CNFD data simulate appropriate temporal dynamics but overestimate
58 streamflow. This suggests that regional unimpaired flow estimates combined with local bias-
59 correction could provide a mechanism to apply ADFs in watersheds without local numerical
60 models.

61
62 **Graphical Abstract**

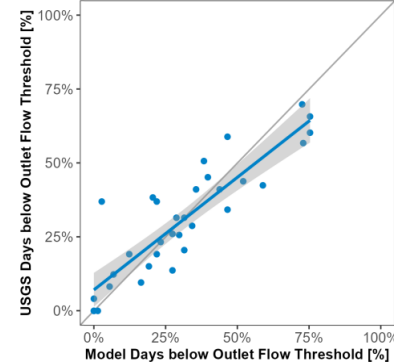
Analytical depletion functions (ADFs) are simple tools to estimate streamflow depletion caused by groundwater pumping



We show that stream drying changes the timing of streamflow depletion and simulate this using ADFs.



ADF simulated streamflow closely matches stream gauging data and output from a local integrated hydrologic model.



63
64

65 **Keywords:** streamflow depletion, groundwater pumping, non-perennial streams, groundwater-
66 surface water interactions, California, SGMA, integrated water resources management

67

68 1. Introduction

69 While surface water and groundwater resources have historically been managed and
70 regulated separately (Gage & Milman, 2020), in many settings they are a single interconnected
71 resource (Winter et al., 1998). Reductions in streamflow caused by groundwater pumping,
72 known as ‘streamflow depletion’ (Barlow et al., 2018; Barlow & Leake, 2012), are a primary
73 mechanism by which groundwater use can affect surface water resources and groundwater-
74 dependent ecosystems (Rohde et al., 2017). In recent decades, water management frameworks
75 have emerged which require quantifying and accounting for interconnections between
76 groundwater and surface water, such as streamflow depletion, when developing water
77 management plans. For example, the European Water Framework Directive and the Australian
78 National Water Initiative both specify that groundwater use cannot impair interconnected surface
79 water resources (Kallis & Butler, 2001; Rohde et al., 2017; Ross, 2018; Vázquez-Suñé et al.,
80 2006). In the United States, California’s Sustainable Groundwater Management Act (SGMA)
81 was passed in 2014, requiring specific priority groundwater subbasins to achieve groundwater
82 sustainability by 2040. SGMA defines sustainability as long-term groundwater management
83 which prevents significant and unreasonable undesirable results, including the depletion of
84 interconnected surface waters (Harter, 2020; Leahy, 2016; Owen et al., 2019). Under SGMA,
85 groundwater managers are expected to estimate the location, timing, and quantity of streamflow
86 depletion occurring due to groundwater pumping (California Department of Water Resources,
87 2024).

88 Quantifying streamflow depletion is challenging because pumping impacts are frequently
89 obscured by other causes of variability such as weather/precipitation dynamics, surface water
90 impoundments/diversions, and lags between groundwater pumping and streamflow impacts
91 (Barlow & Leake, 2012). Streamflow depletion can only be directly measured using
92 observational data at the scale of a stream reach over short timescales (Flores et al., 2020; Hunt
93 et al., 2001; Kollet & Zlotnik, 2003; Malama et al., 2024; Nyholm et al., 2002). However, due to
94 the intensity of data requirements, streamflow depletion cannot be quantified using solely
95 observational data at management-relevant scales such as aquifers or watersheds, and is instead
96 modeled using a variety of approaches (Zipper et al., 2022a). Numerical models, such as
97 MODFLOW, MIKE-SHE, and HydroGeoSphere, simulate stores and fluxes of water in
98 groundwater and surface water systems using physical governing equations (Falke et al., 2011;
99 Fienen et al., 2018; RRCA, 2003; Tolley et al., 2019). Numerical models are generally
100 considered the most reliable tools for assessing streamflow depletion due to their process-based
101 foundation and opportunity for site-specific calibration. Due to their complexity they also have
102 high development costs in terms of data, effort, and expertise (Barlow & Leake, 2012; Zipper et
103 al., 2022a).

104 Analytical depletion functions (ADFs) have been proposed as a low-cost and scalable
105 approach for estimating streamflow depletion (Zipper et al., 2019). ADFs are based on analytical
106 models for streamflow depletion, which mathematically simplify physical governing equations
107 by adopting assumptions, commonly including a well pumping in a homogeneous subsurface
108 connected to a single stream partially or fully penetrating into the aquifer system (Glover &

109 Balmer, 1954; Hantush, 1965; Huang et al., 2018; Hunt, 1999). Simplifications in analytical
110 models can introduce uncertainty, for example by neglecting spatial heterogeneity in the
111 hydrologic response to pumping. ADFs extend analytical models by using empirical approaches
112 to address some of these assumptions, for example by identifying multiple potentially affected
113 stream segments by each well and distributing depletion among stream segments using geometric
114 approaches known as depletion apportionment equations (Zipper et al., 2018; additional details
115 in Section 2). However, a key simplifying assumption that remains is the assumption of an
116 infinite supply of water in the stream. Non-perennial (intermittent or ephemeral) streams are
117 common, estimated to make up more the half the global river network (Messenger et al., 2021),
118 and are becoming increasingly widespread due to climate change and human activities (Sauquet
119 et al., 2021; Trambly et al., 2021; Zipper et al., 2021a). Furthermore, in settings where pumping
120 is a substantial fraction of the water balance, streamflow depletion itself can lead to reductions in
121 stream storage and stream drying (Datry et al., 2022; Malama et al., 2024; Zipper et al., 2022b),
122 which violates the assumption of infinite water.

123 To advance integrated groundwater-surface water decision-making capabilities in
124 watersheds affected by groundwater pumping, this study asks, how does the incorporation of
125 stream drying and the downstream accumulation of streamflow depletion affect the timing of
126 streamflow depletion and the ability of ADFs to simulate spatiotemporal patterns of streamflow
127 and streamflow depletion? To accomplish this, we compare ADF simulations of streamflow and
128 streamflow depletion to observed streamflow data and output from the process-based Scott
129 Valley Integrated Hydrologic Model (SVIHM; Foglia et al., 2013, 2018; Tolley et al., 2019) in
130 the Scott River Valley (California, USA). We develop a novel and simple water budget-based
131 approach to represent stream drying when coupled with ADFs. We thus account for temporal
132 shifts in streamflow depletion caused by stream network drying and can propagate both pumping
133 and drying impacts through the river network. We also demonstrate how a regional statistical
134 model of unimpaired streamflow provides a potential approach for ADF implementation in
135 ungauged and unmodeled watersheds.

136

137 **2. Analytical depletion function (ADF) theory and development**

138 Analytical depletion functions have three primary steps to estimate the impacts of
139 groundwater pumping on streamflow (Figure 1a), which are described in Zipper et al. (2019).
140 First, ‘stream proximity criteria’ are used to identify the stream segments that could be affected
141 by a well based on stream network geometry (Zipper et al., 2019). Second, ‘depletion
142 apportionment equations’ distribute depletion among the affected segments using stream network
143 geometry (Huggins et al., 2018; Reeves et al., 2009; Zipper et al., 2018). Third, streamflow
144 depletion is calculated separately for each affected stream segment using an analytical model
145 (Glover & Balmer, 1954; Hantush, 1965; Hunt, 1999) and scaled based on the apportioned
146 depletion from step two. The resulting output is a three-dimensional streamflow depletion
147 response matrix (White et al., 2021) that quantifies the individual response of each stream
148 segment to each pumping well at each simulated timestep. The impacts of multiple wells are

149 assumed to be linearly additive. Each step can be carried out using different algorithms, and the
150 specific methods used for each of these steps in this study are described in Section 3.4.

151 Past work has evaluated multiple different approaches for each of these steps via
152 comparison to numerical models in a variety of hydrogeological settings including coastal
153 California, coastal and interior British Columbia, and the U.S. High Plains aquifer region (Li et
154 al., 2020; Zipper et al., 2018, 2019, 2021b). This work has shown that ADF and numerical model
155 simulations largely agree for several aspects of pumping impacts on stream networks, including
156 identifying the segment with the greatest streamflow depletion by a given well, the magnitude of
157 depletion in that segment, and the overall spatial distribution and magnitude of depletion across
158 all affected stream segments (Li et al., 2022; Zipper et al., 2019). However, this past work has
159 only used intermodel comparisons for accuracy assessment and has not included any direct
160 comparison to observational data, such as streamflow from gauging stations. Additionally, these
161 evaluations focused on segment-resolution changes in stream-aquifer flux rather than the
162 accumulated streamflow depletion within the stream network and do not account for limited
163 surface water supply (stream drying).

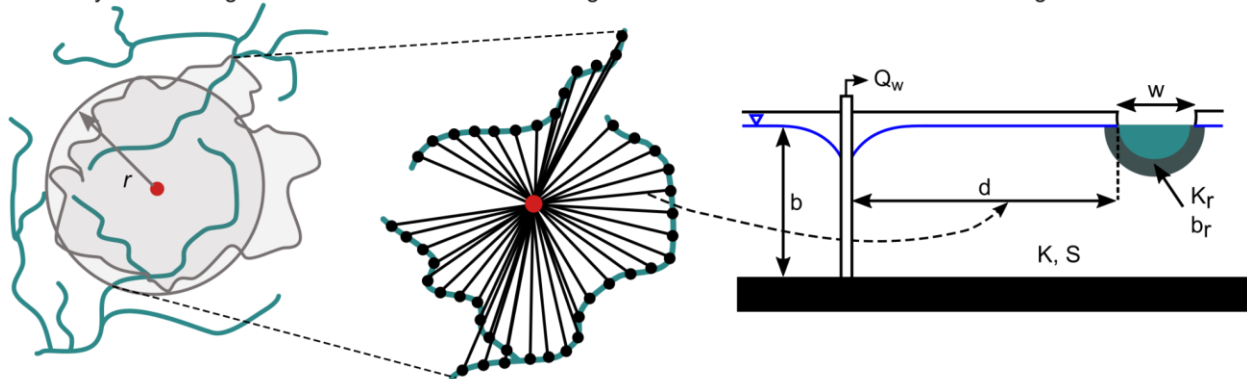
164 In this study, we advance the development of ADFs through two interlinked process
165 representations: (i) the routing of streamflow and streamflow depletion through the stream
166 network, and (ii) stream drying, which leads to a redistribution of depletion in time and space
167 (Figure 1b). To accomplish this, we defined the stream network as a directed graph, with each
168 stream segment represented by a node. To account for potential drying at a given segment, we
169 incorporated an estimate of the streamflow that would have occurred in a segment if there were
170 no groundwater irrigation, which we refer to as “water available”.

171 Combining the two steps, for each timestep, the resulting streamflow is calculated as the
172 difference between water available and ADF depletion if and only if the calculated cumulative
173 depletion by the ADFs in that segment and in upstream segments is less than the water available.
174 If the depletion exceeds the amount of water available, the depletion is assumed to dry the stream
175 and any calculated depletion exceeding water available is “banked” for a later timestep in the
176 same stream segment.

177 Once additional water is available in the stream, banked streamflow depletion is added to
178 the calculated depletion for each timestep, but only up to the water available for depletion in the
179 segment. Thus, a timeseries of redistributed depletion is generated. For each simulated timestep,
180 streamflow and streamflow depletion are calculated starting from headwater segments and
181 moving downstream through the stream network so that any temporal redistributions of
182 streamflow depletion are propagated to downstream segments. This approach to depletion
183 routing and stream drying adopts several assumptions, including that pumping impacts can
184 propagate from upstream to downstream in the stream network within the length of a timestep,
185 and that accurate information about segment-resolution water available can be obtained for each
186 timestep. Details for how these steps are specifically implemented for our study domain are
187 provided in Section 3.

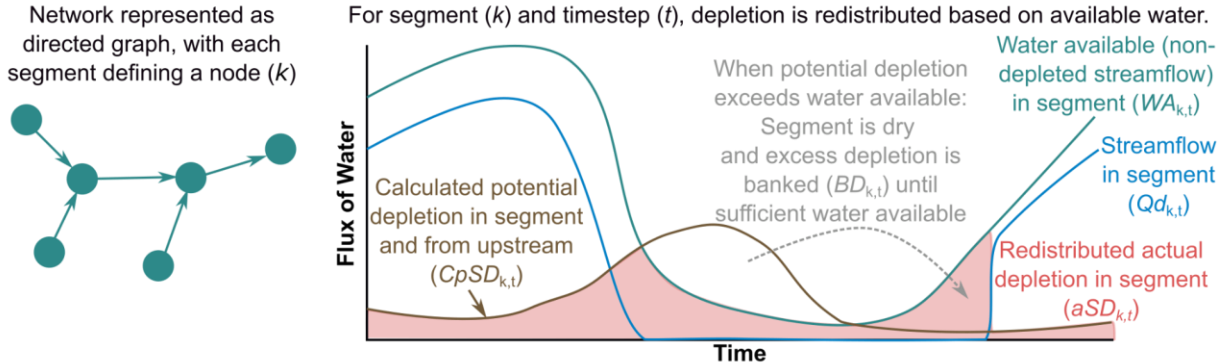
(a) Analytical depletion function workflow

- (1) *Stream Proximity Criteria: Adjacent + Expanding*
Identify affected segments
- (2) *Depletion Apportionment: Web Squared*
Calculate fractional depletion for each segment
- (3) *Analytical Model: Hunt (1999)*
Calculate volumetric depletion for each segment



(b) Depletion routing and stream drying

- (4) *Stream network routing*
Network represented as directed graph, with each segment defining a node (k)
- (5) *Stream drying and depletion redistribution*



Streamflow ($Qd_{k,t}$) calculated as water available ($WA_{k,t}$) minus actual depletion ($aSD_{k,t}$).

188
189 Figure 1. (a) Overview of analytical depletion functions (ADFs) and (b) methods for incorporating depletion routing
190 and stream drying into ADFs. The specific equations and variables used in the figure are defined in Section 3.4.
191

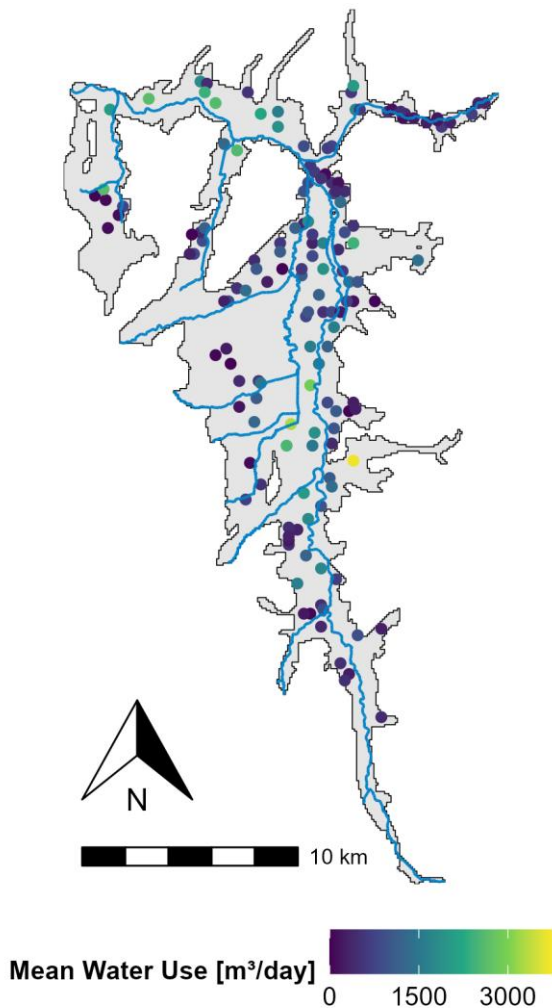
192 **3. Methods**

193 In this study, we develop and test ADFs including stream drying and depletion routing via
194 comparison to stream gauging data and a process-based numerical hydrologic model (SVIHM) in
195 the Scott Valley region of California.

196 *3.1 Study domain: Scott Valley, California*

197 Nestled in the Siskiyou mountains in Northern California, Scott Valley is a
198 Mediterranean-climate montane valley 800 m above sea level and approximately 200 km² in area
199 (Tolley et al., 2019). The Scott River runs north through the valley (Figure 2), draining an area
200 approximately 2100 km² and eventually flowing into the Klamath River. Land use in the flat
201 portions of the valley floor is almost entirely agricultural, with alfalfa and pasture land
202 comprising the largest proportions, while the surrounding uplands are largely managed as part of
203 Klamath National Forest. Agricultural irrigation is the primary use of water, as the 500 mm of
204 average precipitation that occurs in the valley falls between October-May, while the primary
205 growing season is April-September.

206 The Scott River provides habitat to a variety of native aquatic fauna, including Chinook
207 salmon and threatened coho salmon. Quantifying streamflow depletion therefore is critical to
208 effective ecohydrological management. In an attempt to protect these aquatic populations,
209 minimum flow requirements (details in Section 4.4.1) have been suggested for the Scott River at
210 the Fort Jones gauge operated by the U.S. Geological Survey (USGS; gauge 11519500). The
211 Scott River at Fort Jones gauge is located immediately downstream of the closed intermontane
212 valley floor (41.64069017°N, 123.015037°W) at the top of a narrower bedrock canyon, and has
213 streamflow records dating back to 1941. The valley floor is underlain by an aquifer made up of
214 fluvial and alluvial deposits of gravels, sands, silts and clays that form a productive aquifer
215 greater than 120 m thick in places (Mack, 1958), underlain by very low permeability,
216 heterogeneous fractured bedrock. This aquifer system is strongly connected to the river system
217 and stream-aquifer exchange is highly spatially and temporally heterogeneous (Tolley et al.,
218 2019).



219 Figure 2. Scott Valley study domain. The grey shaded area is the active SVIHM model domain, which encompasses
220 the valley bottom aquifer. Blue lines show the stream network, with the watershed outlet in the northwest corner of
221 the domain. Pumping wells are colored by their average water use over the period of comparison.
222
223

224 3.2 Scott Valley Integrated Hydrologic Model (SVIHM)

225 SVIHM consists of three models run sequentially: an upper watershed tributary
226 streamflow regression model, a soil-crop-water balance (agricultural water demand) model, and
227 a numerical groundwater-surface water flow model using MODFLOW-NWT (Niswonger et al.,
228 2011). The streamflow regression model predicts inflows into the topographically flat portion of
229 Scott Valley overlying the aquifer system using statistical relationships estimated between the
230 tributary gauges (dependent variable) and the Fort Jones gauge (independent variable). The soil-
231 crop-water balance model estimates surface water and groundwater abstraction using a crop-
232 coefficient based ET estimation and field-scale information about crops, soils, irrigation systems,
233 their efficiency, and water sources (Foglia et al., 2013; Tolley et al., 2019). Recharge to the
234 underlying aquifer system is estimated for each field using a tipping-bucket approach; the
235 method and underlying equations are fully documented in Tolley et al. (2019). The MODFLOW-
236 NWT model simulates the coupled groundwater-surface water system. The model consists of 2
237 layers, 440 rows and 210 columns (19,869 and 14,054 active nodes in layers 1 and 2,
238 respectively), each 100m x 100m in size, and aquifer properties vary spatially via nine
239 contiguous, homogenous hydrogeologic zones (Tolley et al., 2019). The model has monthly
240 stress periods, daily time steps, and uses tab files to input the tributary inflows into the valley on
241 a daily basis.

242 SVIHM has been used as a decision-support tool in Scott Valley for over a decade
243 (Foglia et al., 2013, 2018; Kouba & Harter, 2024; Siskiyou County Water Conservation and
244 Flood Control District, 2021; Tolley et al., 2019). Agricultural water use data are not available in
245 the region, and thus the model serves an important purpose in estimating the valley water use and
246 water balance. Additionally, SVIHM facilitates a wide variety of scenarios to be tested, e.g.,
247 removal/addition of pumping wells, land use changes, irrigation method changes, groundwater
248 and surface water curtailments, droughts, etc. The specific SVIHM scenarios used in this study
249 are described in Section 3.4.3.

250 3.3 California Natural Flows Database (CNFD)

251 The California Natural Flows Database (CNFD) is the result of a modeling approach
252 developed in partnership between the California Environmental Flows Framework
253 (<https://ceff.ucdavis.edu/>) technical team and the U.S. Geological Survey (USGS) that uses
254 machine learning models to predict monthly unimpaired flows across the state of California.
255 Unimpaired flows are a key water resource management consideration, particularly for the
256 conservation of aquatic ecosystems. Modeling the natural flow regime allows for an increased
257 understanding of existing alteration across surface water systems. Zimmerman et al. (2018)
258 identified 250 reference stream gages with minimal flow alteration and divided them into three
259 regions based on climate and hydrologic conditions. Using observed monthly flows, climate and
260 run-off variables, and fixed physical watershed characteristics, they developed random forest
261 statistical models for each region. These random forest models were then applied to predict flows
262 for all streams in the state, estimating natural flow values from 1950 to 2015 at stream segment

263 resolution (based on the resolution of the U.S. National Hydrography Dataset [NHD]), along
264 with the range of uncertainty (Zimmerman et al., 2018).

265 Predictive accuracy of the model was assessed by comparing predicted monthly
266 minimum, mean, and maximum flows to observed flows at randomly selected reference stream
267 gages believed to have natural flows (locations lacking upstream hydrologic alteration). Average
268 model performance results included the ratio of observed to predicted value of 0.94, an r-squared
269 value of 0.80, a percent bias of -3.30 and a Nash-Sutcliffe Efficiency of 0.75 (Zimmerman et al.,
270 2018). Studies have expanded upon this approach, utilizing modeled natural flows to propose
271 ecologically functional flow metrics for riverine ecosystems statewide (Grantham et al., 2022).
272 The CNFD is continuously updated, and monthly unimpaired flow estimates are available up to
273 the present day (<https://rivers.codefornature.org/>). The specific CNFD data used in this study are
274 described in Section 3.4.3.

275 *3.4 ADF implementation to calculate depletion, streamflow, and drying in Scott Valley*

276 3.4.1 Calculating potential streamflow depletion from ADFs

277 ADFs directly calculate the potential streamflow depletion, defined as the amount of
278 streamflow depletion that would occur if the stream had an unlimited supply of water, for each
279 stream segment at each timestep. The primary data sources for ADFs are the hydrostratigraphic
280 parameters of transmissivity and storativity; the locations and pumping schedules for any wells;
281 and the stream network. For our comparison, we used data from SVIHM to parameterize ADFs
282 to maximize input data commensurability for an ‘apples to apples’ comparison. Therefore, our
283 study is intended to understand the differences in simulated streamflow and streamflow depletion
284 that can be attributed to differences in model structure and complexity, rather than differences
285 that may be caused by model input data source or uncertainty. While we do not carry out a
286 formal sensitivity analysis in this study, we do evaluate multiple data sources related to water
287 available to understand the sensitivity of ADF performance to this input data. For transmissivity
288 (Tr), we developed gridded maps by multiplying horizontal hydraulic conductivity (K) by aquifer
289 thickness (b) at each SVIHM grid cell. For storativity (S), we summed specific yield (Sy) and the
290 product of specific storage (Ss) and b . Since Sy is substantially larger than $Ss*b$, variation in S
291 is primarily driven by Sy zones within SVIHM. Pumping locations were defined as the center of
292 each SVIHM grid cell with a pumping well, and pumping schedules (Q_w) were obtained from
293 SVIHM as described in Section 3.2. The stream network was also defined based on the SVIHM
294 grid. We then summarized hydrostratigraphic input parameters for each potential combination of
295 wells and affected streams using the average Tr and S value for any grid cell along a line
296 connecting each well to the closest point on each stream segment.

297 For ADF implementation, we used the ‘adjacent + expanding’ stream proximity criteria
298 (Figure 1a, step 1), which allows wells to affect streams in any adjacent catchment or within a
299 radial distance that expands with time (details in Zipper et al., 2019). The allowable radial
300 distance at each timestep was based on the 10th percentile of S and 90th percentile of Tr for all
301 well-stream pairs. Since low values of S and high values of Tr are generally associated with a
302 greater fraction of pumping from streamflow depletion, these values are meant to represent an

303 inclusive stream proximity criteria and ensure that all potentially impacted streams are identified.
304 For the depletion apportionment equation (Figure 1a, step 2), we used the web-squared approach
305 developed in Zipper et al. (2018) that distributes fractional depletion based on a weighted inverse
306 distance of evenly spaced points along each affected stream segment. Compared to a simple
307 inverse-distance approach, the web squared approach accounts for both the distance from wells
308 to streams as well as the geometry of each stream segment. The ‘adjacent + expanding’ and ‘web
309 squared’ approaches have generally been found to provide the best performance in past studies
310 (Li et al., 2020; Zipper et al., 2018, 2019, 2021b), so we did not conduct additional testing of
311 alternate stream proximity criteria and depletion apportionment equations in this study.

312 To estimate the amount of streamflow depletion due to pumping in each stream segment
313 (Figure 1a, step 3), we used the analytical model developed in Hunt (1999) which simulates a
314 partially-penetrating stream with a streambed layer that impedes flow as a function of its
315 conductance (λ). For the conductance of the streambed layer, we used the λ values in each
316 segment defined in SVIHM. In practice streambed conductance has tremendous fine-scale
317 spatiotemporal variability (Abimbola et al., 2020b, 2020a; Korus et al., 2018, 2020) and is rarely
318 known with any confidence (Christensen, 2000), and therefore this parameter is typically
319 unknown or calibrated. To evaluate the potential impacts of the analytical model selection, we
320 repeated our analysis using the Glover & Balmer (1954) analytical solution that assumes a fully
321 penetrating stream with no resistance to flow and therefore does not require λ . We found that
322 simulated depleted streamflow at the watershed outlet was insensitive to the selection of an
323 analytical model in this domain (Figure S4), and therefore only results from the Hunt model are
324 shown throughout the rest of the manuscript. All ADF simulations were done using a five-day
325 timestep for the period from October 1, 1990 to September 30, 2023 and were implemented
326 using the streamDepletr package for R (Zipper, 2023).

327 3.4.2 Incorporating depletion routing and stream drying

328 The ADF as described in Section 3.4.1 and shown in Figure 1a calculates the potential
329 streamflow depletion, $pSD_{k,t}$ at each stream segment k and time-step t , with no regard to whether
330 there is sufficient water in the stream to meet this demand. In this section, we describe how
331 incorporating the water available in each segment at each timestep ($WA_{k,t}$) allows us to calculate
332 the estimated depleted streamflow ($Qd_{k,t}$) and actual streamflow depletion ($aSD_{k,t}$) for each
333 segment and timestep (five days) as shown in Figure 1b. To do this, we consider that each stream
334 segment has a “memory” of the amount of potential streamflow depletion that could not actually
335 occur due to lack of instream flow, which we define as the banked depletion (BD). Initially, BD_k
336 for each segment is zero. BD_k increases whenever $pSD_{k,t}$ exceeds $WA_{k,t}$, which occurs when
337 instream flows are insufficient for the streamflow depletion demand. BD_k decreases when BD_k is
338 greater than 0 and $pSD_{k,t}$ is less than $WA_{k,t}$, which occurs when there is both banked depletion
339 and water available in the stream beyond simulated potential depletion. Specifically, the
340 following algorithm is used to compute streamflow depletion (aSD) and streamflow (Qd) for
341 each segment k and time t :

- 342 ● Using the directed graph stream network (Figure 1b), aSD in time-step t upgradient of
 343 segment k is summed and added to the $pSD_{k,t}$ to provide the ‘cumulative potential
 344 streamflow depletion’ $CpSD_{k,t}$ in a segment:

345
$$CpSD_{k,t} = pSD_{k,t} + \text{sum}[aSD_t \text{ for all segments upstream of } k] \quad \{\text{Eq. 1}\}$$

- 346 ● If $CpSD_{k,t} \leq WA_{k,t}$, then:
 347 ○ The actual streamflow depletion, $aSD_{k,t}$, equals the cumulative potential
 348 streamflow depletion plus any accumulated banked depletion, $BD_{k,t}$ (see below),
 349 up to the amount of water available in the stream:

350
$$aSD_{k,t} = \min[(CpSD_{k,t} + BD_{k,t}), WA_{k,t}] \quad \{\text{Eq. 2}\}$$

- 351 ○ For the following time-step, $BD_{k,t+1}$ is then adjusted by the amount of delayed
 352 depletion that occurred in time-step t , unless it is zeroed out:

353
$$BD_{k,t+1} = \max[0, (BD_{k,t} - (aSD_{k,t} - CpSD_{k,t}))] \quad \{\text{Eq. 3}\}$$

- 354 ● Else, if $CpSD_{k,t} > WA_{k,t}$, then:
 355 ○ The actual streamflow depletion is equal to the amount of water available and the
 356 stream has dried:

357
$$aSD_{k,t} = WA_{k,t} \quad \{\text{Eq. 4}\}$$

- 358 ○ The amount of potential streamflow depletion that did not occur is added to the
 359 accumulated delayed depletion available in the next time step, $BD_{k,t+1}$:

360
$$BD_{k,t+1} = BD_{k,t} + (CpSD_{k,t} - WA_{k,t}) \quad \{\text{Eq. 5}\}$$

- 361 ● For each timestep, the depleted streamflow is then calculated as the difference between
 362 water available and actual streamflow depletion:

363
$$Qd_{k,t} = WA_{k,t} - aSD_{k,t} \quad \{\text{Eq. 6}\}$$

- 364 ● Calculations are done sequentially, starting at the headwaters (nodes in the directed graph
 365 that do not have any inflowing segments) and moving downstream so that the actual
 366 streamflow depletion following banking and redistribution ($aSD_{k,t}$) propagates
 367 downwards to influence the timing of streamflow and depletion in downstream segments.

368 3.4.3 Defining water available

369 Incorporation of depletion routing and stream drying requires input data on the amount of
 370 water available, which is the streamflow that would have occurred without pumping. For this
 371 study, we compared two different water available sources: SVIHM and CNFD. The simulations
 372 using SVIHM to simulate water availability are intended to maximize commensurability with
 373 SVIHM estimated streamflow depletion, allowing us to understand the differences between
 374 observed streamflow, SVIHM, and ADFs when the non-depleted streamflow is well-known. The
 375 use of CNFD data is intended to test the potential applicability to watersheds that do not have

376 locally-developed estimates of non-depleted streamflow to help understand potential applications
377 of ADFs for unmodeled regions.

378 From SVIHM, we used output from two specific SVIHM simulations: the calibrated
379 basecase (#1 in Table S1), with historical land use and water withdrawals for the period from
380 10/1/1990 to 9/30/2023; and a no-groundwater-irrigation scenario (#3b in Table S1), in which all
381 model parameters and inputs are the same except that there is no groundwater pumping and
382 groundwater-irrigation-dependent crops are replaced by natural vegetation. For ADF
383 implementation, we used the segment-scale results of the SVIHM no-groundwater-irrigation
384 scenario as our water available input. In SVIHM, we compared differences between these two
385 scenarios to quantify the magnitude of streamflow depletion caused by groundwater pumping
386 (Barlow & Leake, 2012; Zipper et al., 2022a). Other factors causing streamflow variability and
387 groundwater-surface water exchange are identical to the basecase (including weather variability,
388 surface water diversions, land use practices associated with surface water irrigation, etc). Hence,
389 the differences between these two scenarios provide the hydrologic response to both changes in
390 pumping and associated differences in the water balance that occur as a result of land use
391 reverting to natural vegetation due to the lack of groundwater irrigation (Kouba & Harter, 2024).
392 For our segment-resolution evaluation of ADF performance, we also compared ADF output with
393 water available defined using an additional SVIHM scenario in which there was no groundwater
394 pumping, but land use practices stayed the same throughout the watershed (i.e., groundwater-
395 irrigated fields reverted to rainfed agriculture; scenario #2 in Table S1). While this is not a
396 realistic agricultural practice for the region, this comparison allowed us to isolate the direct
397 effects of pumping on streamflow, ignoring other changes to the water balance associated with
398 conversion of groundwater-irrigated fields to natural vegetation. To assess the overall influence
399 of the SVIHM scenario used for defining water available, we tested nine different SVIHM model
400 configurations (Table S1, Figure S5, Figure S6). All SVIHM simulations used the version of the
401 model calibrated and described by Tolley et al. (2019).

402

403 Table 1. Model simulations compared in this study.

Name	Streamflow depletion model	Water available source	Consideration of stream drying
ADF + SVIHM, No Drying	ADF	SVIHM, no irrigation in groundwater-dependent cropland scenario (#3b in Table S1)	No
ADF + SVIHM + Drying	ADF	SVIHM, no irrigation in groundwater-dependent cropland scenario (#3b in Table S1)	Yes
ADF + CNFD, No Drying	ADF	CNFD v2.1.1	No
ADF + CNFD + Drying	ADF	CNFD v2.1.1	Yes
SVIHM	SVIHM basecase with historical irrigation and land use (#1 in Table S1)	SVIHM, no irrigation in groundwater-dependent cropland scenario (#3b in Table S1)	Yes

404

405 To assess the potential for ADF applications in locations without locally calibrated
 406 streamflow models, we used data from version 2.1.1 of the CNFD database as water available
 407 input for ADFs. This version of CNFD has a Nash-Sutcliffe Efficiency > 0.9 for the 2010-2021
 408 period via comparison to reference gages around the state, though reference gages are largely not
 409 available for northern portions of the state such as the Scott Valley area. We extracted monthly
 410 CNFD predicted flow for the October 1990 to September 2023 study period at each NHD
 411 segment in the study domain. In some parts of the study domain, the NHD stream segments used
 412 in CNFD were more finely discretized than the MODFLOW stream segments used by SVIHM
 413 (i.e., < 100 m resolution). For these segments, we averaged the predicted unimpaired flow from
 414 CNFD segments to match the spatial scale of SVIHM. This produced a timeseries of monthly
 415 CNFD unimpaired flow at the same spatial resolution of SVIHM. Since CNFD does not
 416 incorporate surface water diversions (which are not simulated by ADFs), we then subtracted out
 417 estimated surface water diversions from SVIHM at each segment. Therefore, the ADF + CNFD
 418 simulations provide an evaluation of the potential for ADFs to estimate streamflow depletion in
 419 settings where non-depleted streamflow is unknown, but estimates of surface water diversions
 420 have been developed.

421 For each water available source, we compared ADF simulations without stream drying
 422 (i.e., only steps shown in Figure 1a and described in Section 3.4.1) and with stream drying (i.e.,
 423 including steps shown in Figure 1b and described in Section 3.4.2). The full collection of
 424 scenarios is described in Table 1.

425 3.5 ADF model evaluation

426 To evaluate the performance of the ADFs and the importance of incorporating stream
427 drying into these models, we compared a variety of variables for each model configuration in
428 Table 1. To evaluate the ability to simulate streamflow, we compared streamflow simulated by
429 ADFs and SVIHM with observations from the USGS streamflow gauging station at the
430 watershed outlet. This was primarily done at the model output timestep (5-day), though we also
431 tested fit for monthly/annual average streamflow and the number of days streamflow dropped
432 below important management thresholds. Since low flows are of particular management interest
433 in this domain due to their impact on salmonid habitat, we used log-transformed streamflow,
434 referred to as log(Streamflow), for our comparison. For the calculation of fit statistics when
435 streamflow was equal to 0, we added a small value (1% of the minimum observed streamflow) to
436 avoid infinite log(Streamflow) values. Beyond streamflow, at the watershed outlet we compared
437 the total depletion at each timestep between ADFs and SVIHM. To evaluate performance
438 throughout the network, we also compared segment-resolution streamflow and streamflow
439 depletion between the ADFs and SVIHM.

440 We calculated fit statistics including the Kling-Gupta Efficiency (KGE; Gupta et al.,
441 2009), coefficient of determination (R^2), and root mean squared error as a percentage of the
442 range of observed streamflow values (normalized RMSE). The KGE is a fit statistic that
443 integrates bias, correlation, and relative variability between simulated and observed values , with
444 a KGE of 1.0 indicating a perfect agreement between simulated and observed data and $KGE < -$
445 0.41 indicating that using the mean of the observational data would be a better fit than the model
446 (Knoben et al., 2019). The R^2 represents the overall degree of correlation between the model and
447 observations. The normalized RMSE provides an indication of the degree of error in proportion
448 to the magnitude of observed variability.

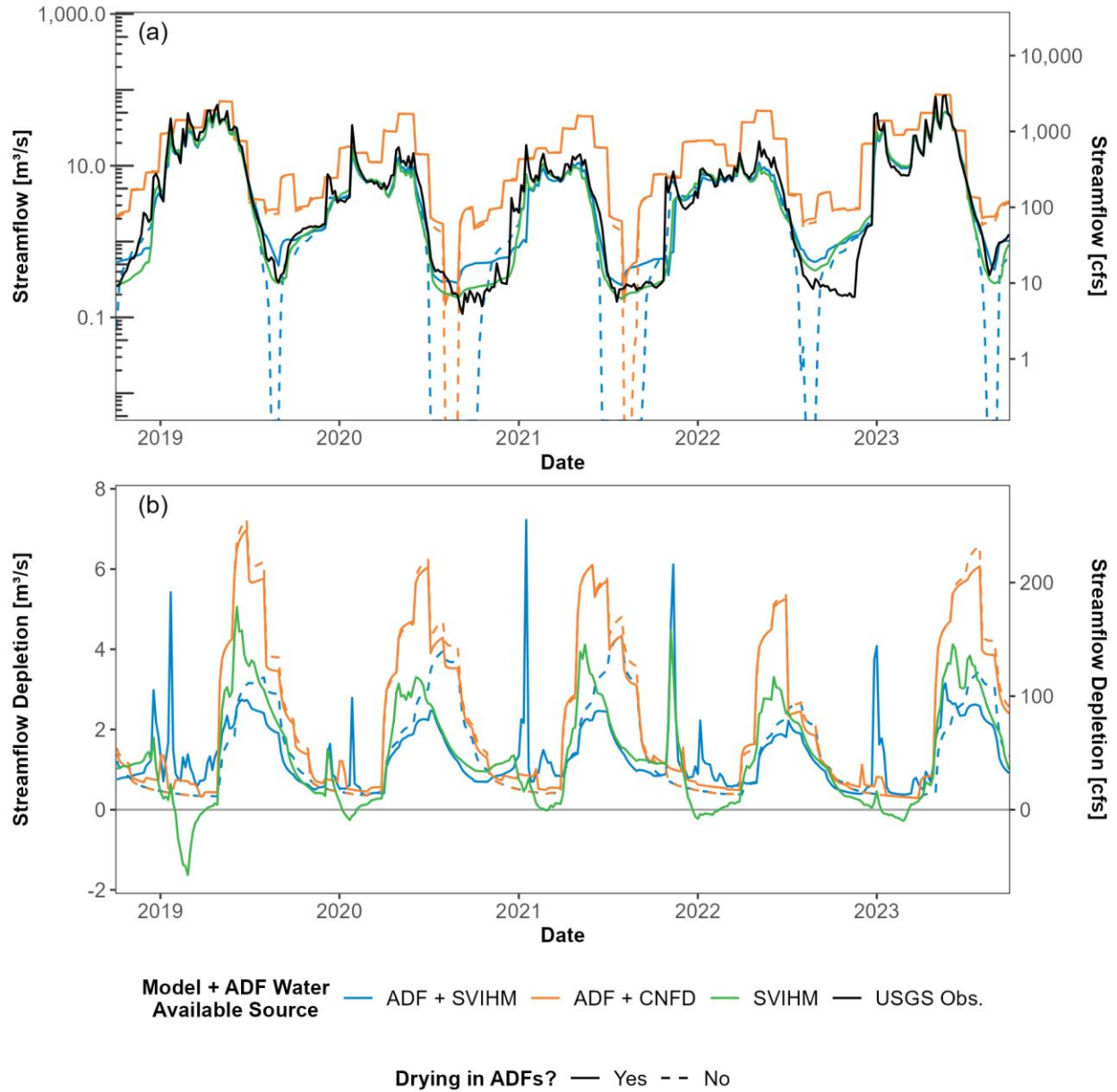
449 4. Results and Discussion

450 4.1 Simulating streamflow and streamflow depletion at the watershed outlet

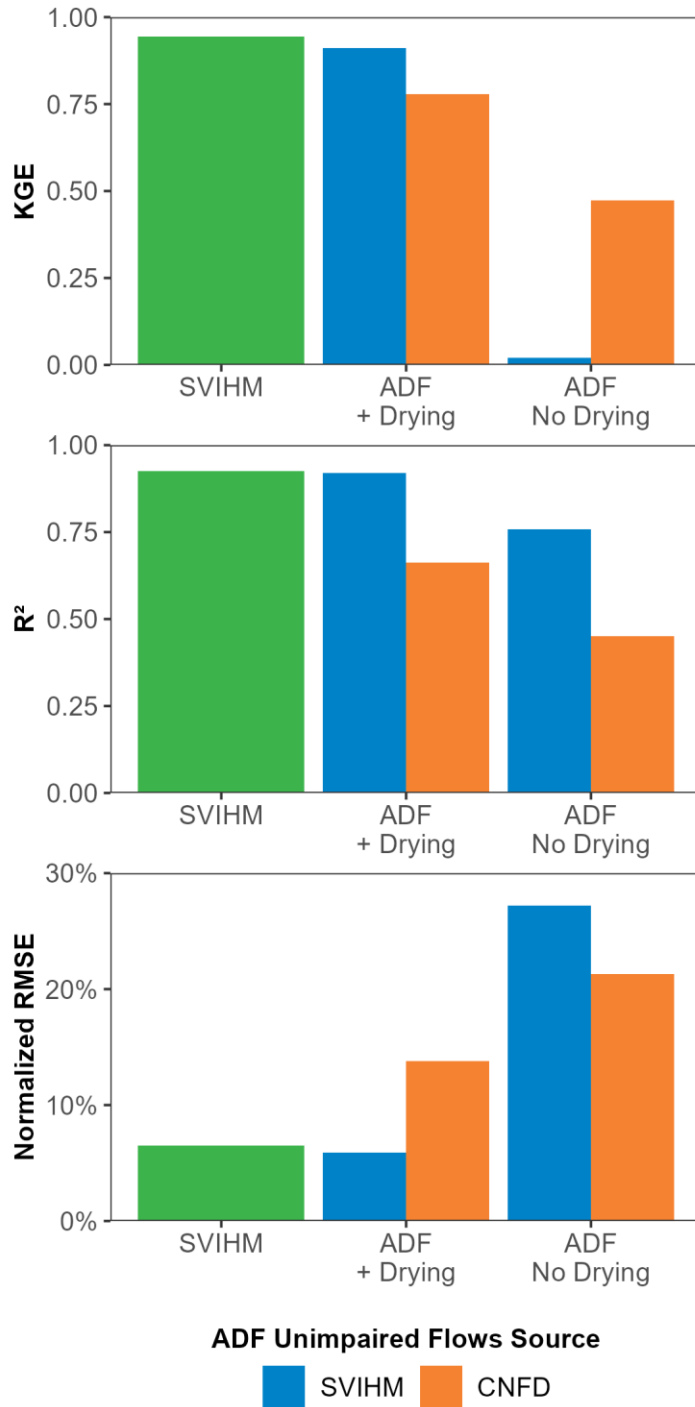
451 The ADF + SVIHM models were able to accurately simulate both streamflow (Figure 3a,
452 Figure S1) and streamflow depletion (Figure 3b, Figure S2) when drying was included. Across
453 most years, ADFs without drying underestimate streamflow and overestimate streamflow
454 depletion during summer and early fall, and as a result incorrectly predict that the stream should
455 dry at the watershed outlet during the summer. In contrast, the ADF + SVIHM + Drying models
456 accurately simulate the depletion of flow without drying across all years (Figure 3a). Overall, the
457 performance of the ADF + SVIHM + Drying models for simulating for log(Streamflow),
458 assessed via comparison to the USGS stream gauging data, is comparable to the performance of
459 SVIHM (Figure 4). The ADF + SVIHM + Drying models have a KGE of 0.91 (compared to 0.94
460 for SVIHM), an R^2 of 0.92 (compared to 0.93 for SVIHM), and a normalized RMSE of 5.9%
461 (compared to 6.5% for SVIHM). The ADF + SVIHM, No Drying models have substantially
462 worse agreement with observations (KGE of 0.02, R^2 of 0.76, normalized RMSE of 27.2%),
463 highlighting the strong improvements in ADF performance from the incorporation of stream
464 drying.

465 Due to their lower data requirements relative to numerical models, ADFs are potentially
466 useful for water management decision support in settings without existing integrated
467 groundwater-surface water models (Huggins et al., 2018; Li et al., 2022). Our ADF + CNFD
468 simulations provide one opportunity to evaluate their potential application in these settings. We
469 found that the ADF + CNFD models, which define water available based on the statewide
470 unimpaired flow model, effectively captured temporal patterns of streamflow and streamflow
471 depletion, but streamflow is biased high (Figure 3). The ADF + CNFD models were
472 parameterized using calibrated hydrostratigraphic parameters from SVIHM to maximize the
473 commensurability of the comparison, and absent this information, may have performed
474 differently (see Section 4.4.2 for more discussion of ADF parameterization and uncertainty). The
475 ADF + CNFD model results also have a blockier pattern because the CNFD is a monthly model,
476 unlike the daily SVIHM output.

477 The high bias in depleted streamflow in the ADF + CNFD model occurs because
478 unimpaired flow estimates from the CNFD model tend to be higher than the SVIHM no-
479 groundwater-irrigation scenario (Figure S5), which may result from several factors. The first is
480 that the two models are not designed to simulate the same thing. The SVIHM no-groundwater-
481 irrigation scenario still includes agricultural land cover in areas of the domain where irrigation is
482 supplied by direct surface water diversions, while the CNFD is meant to represent unimpaired
483 flow under a natural vegetation land cover and unaltered land use (though the volume of the
484 diversions is subtracted out). Non-irrigated agricultural land and an unaltered landscape without
485 modifications such as ditching would likely produce differences in the timing and magnitude of
486 fluxes such as groundwater recharge and evapotranspiration that can lead to differences in
487 streamflow, even in the absence of pumping. To assess this potential driver of differences, we
488 compared CNFD to additional SVIHM model scenarios with a variety of different natural
489 vegetation parameterizations. We found that the SVIHM natural vegetation scenarios still had a
490 lower simulated streamflow than CNFD (Figure S5). A second potential reason for disagreement
491 between these two models could be that the CNFD is trained on reference watersheds across the
492 state (Zimmerman et al., 2018), most of which are watersheds discharging from mountain
493 regions without upstream alluvial valleys. Therefore, it is possible that the important
494 hydrological processes in the Scott Valley are outside the range of training watersheds and may
495 have different dynamics that are not well-captured by CNFD. Finally, we would generally expect
496 SVIHM to be more accurate for the Scott Valley because it is locally calibrated, while CNFD is a
497 statewide model. It may be possible to mitigate the high bias of CNFD or other unimpaired flow
498 models through approaches such as regional bias-correction or ADF calibration, which are not
499 tested in this study but discussed in Section 4.4.2.



500
 501 Figure 3. Comparison of ADFs to stream gauge and numerical model data at the watershed outlet over the last 5
 502 years of the study period. (a) Streamflow. (b) Streamflow depletion. The USGS Obs. data is not included in panel
 503 (b) because streamflow depletion cannot be quantified from observational data alone. Results from all 33 study years
 504 are shown in Figure S1 and S2.
 505



506
 507
 508
 509
 510

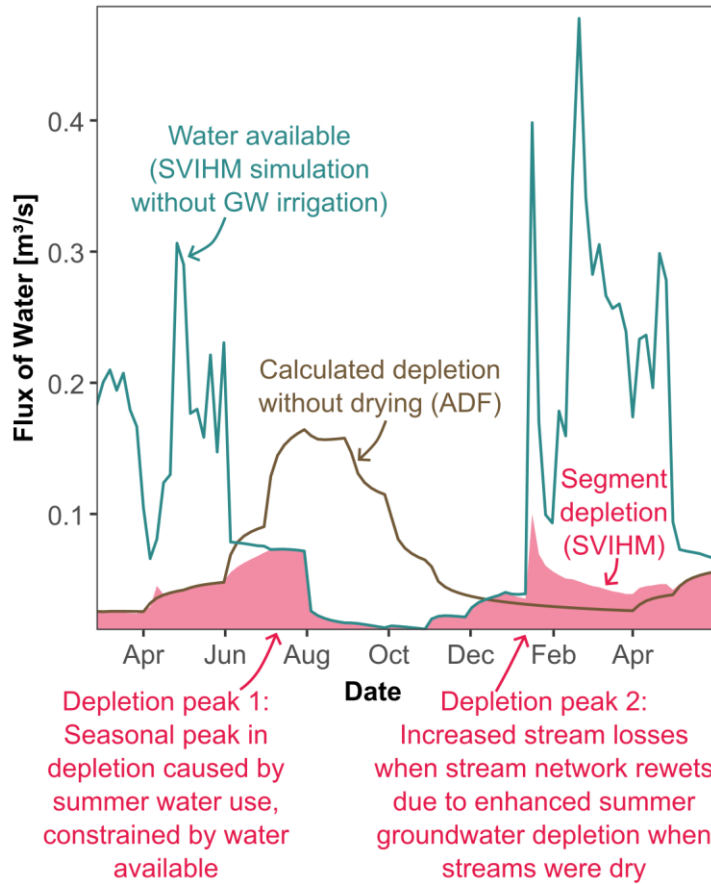
Figure 4. Model fit metrics for daily log(Streamflow), for SVIHM and ADFs with and without drying, calculated via comparison to USGS gauge at the watershed outlet. Normalized RMSE is the RMSE divided by the range of observed values. For fit statistics based on water year type, see Figure S3.

511 *4.2 Impacts of stream drying on timing and magnitude of streamflow depletion*

512 The ADF models including stream drying have better agreement with observations
513 compared to the no drying models (Figure 3, Figure 4). Simulating stream drying is critical
514 because upstream flow intermittency can lead to delays in the manifestation of streamflow
515 depletion at the watershed outlet, even if the outlet itself does not dry, due to changing stream
516 connectivity and storage dynamics within the stream network. This can lead to a behavior in
517 which there are multiple peaks in streamflow depletion within a year, including outside the
518 pumping season (Figure 3b), which has not to our knowledge been described in the literature.

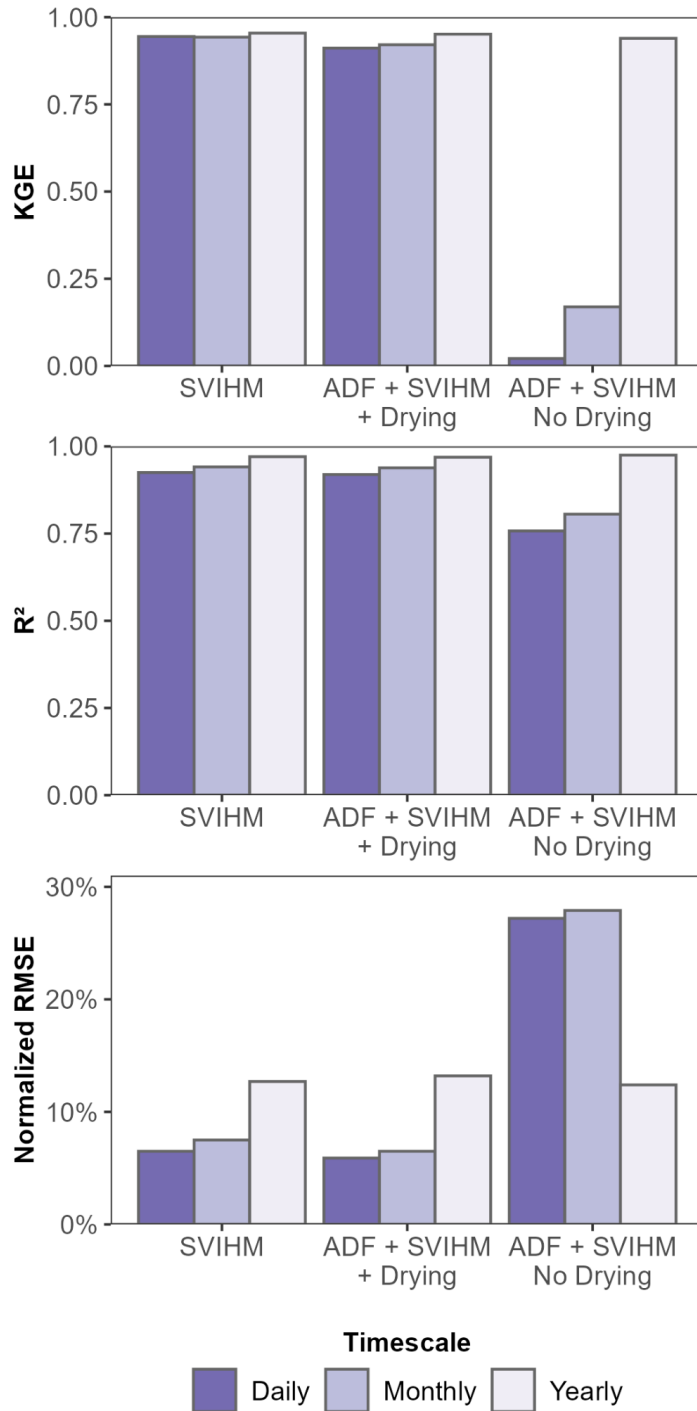
519 Mechanistically, the multiple streamflow depletion peaks are caused by changes in
520 hydrologic connectivity in both the longitudinal (upstream-downstream stream network
521 disconnection) and vertical (stream-aquifer) dimensions. In the Scott Valley, the first streamflow
522 depletion peak occurs early in the pumping season, when seasonal pumping has led to the onset
523 of streamflow depletion in the watershed but there is still sufficient surface water available from
524 snowmelt (Peak 1 in Figure 5). This pumping steadily depletes streamflow until drying occurs,
525 typically first in relatively small tributaries flowing into the main stem of the river, at which
526 points these tributaries become longitudinally disconnected from the outlet. Once the stream
527 network starts to dry, additional pumping leads primarily to groundwater depletion, rather than
528 streamflow depletion, and the water table drops below where it would have been in a non-
529 pumped condition. As a result, once fall/winter rains begin and the stream network starts to
530 rewet, there is enhanced infiltration through the streambed in order to refill groundwater storage
531 and reconnect the stream to the aquifer (peak 2 in Figure 5). These changes in hydrologic
532 connectivity are explicitly simulated in the process-based SVIHM and reasonably reproduced in
533 the simple ADF water budget approach developed in this study (Figure 1b). Since the primary
534 impacts of drying are changes in the timing (but not total volume) of streamflow depletion,
535 incorporating these dynamics is important to accurately simulate daily and monthly average
536 streamflow, but not influential for annual streamflow estimates (Figure 6).

537 The timing of stream drying and rewetting, and related changes in stream connectivity,
538 are critically important for local aquatic ecosystems and downstream water users (Price et al.,
539 2021, 2024). In the Scott River, the timing of the transition from the dry to wet season is a key
540 ecohydrological process supporting local salmonid populations (Kouba & Harter, 2024). Since
541 stream intermittency is globally widespread, particularly in semi-arid to arid regions where
542 irrigated agriculture is common (Hammond et al., 2021; Messenger et al., 2021; Shanafield et al.,
543 2021), it suggests these lagged depletion peaks during stream rewetting may be a common
544 phenomena that require explicit consideration when developing integrated groundwater and
545 surface water management plans (Lapides et al., 2022). The water budget-based method we
546 developed provides a parsimonious approach that appears to work well in seasonally dry
547 watersheds like the Scott River Valley. In watersheds with different drying regimes (Price et al.,
548 2021), particularly those with multi-year shifts between dry and wet regimes driven by
549 interconnections between alluvial and regional aquifer systems (Zipper et al., 2022b), additional
550 evaluation is needed to determine whether this approach is suitable.



551

552 Figure 5. Example illustrating multiple streamflow depletion peaks, which forms the basis for the ADF
 553 implementation of drying in Figure 1b. The blue line shows the SVIHM no-groundwater-irrigation scenario, which
 554 defines water available, and the red shading shows the difference between the SVIHM no-groundwater-irrigation
 555 scenario and basecase scenario, illustrating the double peak dynamics in the process-based numerical model. The
 556 brown line shows ADF estimated depletion without drying to illustrate what depletion would have been in the
 557 absence of stream drying. Data shown here are for Patterson Creek, a tributary to the Scott River on the west side of
 558 the study domain, for the March 2020 to May 2021 period. SVIHM scenarios are detailed in Table S1.
 559



560

561 Figure 6. Model fit metrics based on timescale of comparison for log(Streamflow), for SVIHM and ADFs with and
 562 with drying, calculated via comparison to USGS gauge at the watershed outlet. ADFs shown here are using the
 563 SVIHM no-groundwater-irrigation scenario as available water. Normalized RMSE is the RMSE divided by the
 564 range of observed values. The Yearly fit is calculated as April-March average streamflow, based on the timing of the
 565 onset of seasonal pumping in the watershed.
 566

567 *4.3 Simulating streamflow and streamflow depletion throughout the watershed*

568 To evaluate the accuracy and utility of ADFs throughout the Scott Valley watershed,
569 including in settings where there was no stream gauging data available, we compared segment-
570 resolution ADF + SVIHM + Drying output to results from SVIHM. We excluded stream
571 segments where SVIHM results indicated depletion was $< 1\%$ of non-depleted streamflow $>$
572 90% of the time to focus only on locations with substantial pumping impacts. We found that
573 agreement between the two modeling approaches was generally good ($KGE > 0$) to excellent
574 ($KGE > 0.5$) for $\log(\text{Streamflow})$ when using the SVIHM no-groundwater-irrigation scenario to
575 define ADF water available (Figure 7a). Agreement in terms of streamflow depletion (Figure 7b)
576 was worse than agreement for streamflow, primarily in tributary regions, but generally had KGE
577 > 0.5 along the main stem of the Scott River.

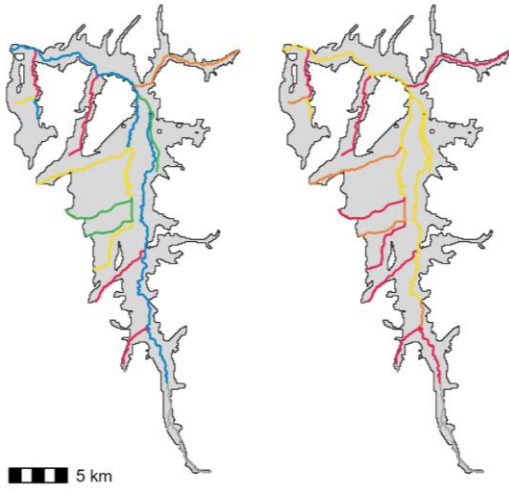
578 While our primary comparisons between the ADFs and SVIHM used output from
579 SVIHM that modified pumping and land use simultaneously (scenario #3b from Table S1), we
580 also compared streamflow depletion using an alternate SVIHM parameterization, in which
581 pumping was turned off but groundwater-irrigated areas remained in agricultural land cover
582 (scenario #2 from Table S1). This is not a realistic representation of feasible land use practices in
583 the Scott Valley, since groundwater-supported agriculture would likely revert to non-agricultural
584 land cover if irrigation was unavailable, but rather a model experiment that allows us to isolate
585 the impacts of groundwater pumping on streamflow in SVIHM to provide a more commensurate
586 comparison to ADF results which directly simulate the impacts of pumping (not land use change)
587 on streamflow. We found that agreement in simulated streamflow depletion was much stronger
588 using scenario #2 compared to scenario #3b (Figure 7d), with only a slight degradation in
589 simulated streamflow (Figure 7c). This comparison among SVIHM scenarios highlights the need
590 for segment-level management decision-making to consider the full suite of hydrologic changes
591 associated with land use and water management decisions. Since ADFs directly simulate
592 streamflow depletion caused by changes in pumping and do not simulate other changes in the
593 water balance associated with conversion between natural and agricultural land cover, it suggests
594 that ADF performance could be further improved by developing complementary approaches to
595 assess holistic changes to the water balance associated with pumping decisions, such as
596 differences in recharge, infiltration, and runoff. If independent estimates of changes in
597 consumptive water use could be developed (for example, through approaches like remote sensing
598 of evapotranspiration; Asarian et al., 2025), these water balance changes could be integrated with
599 ADF-based estimates of pumping impacts on streamflow to provide a full accounting of changes
600 in the water balance and impacts on streamflow.

601 Agreement for both streamflow and streamflow depletion tends to be best for the higher-
602 streamflow and more heavily-depleted segments along the main stem (Figure 7, Figure S7) and
603 worst in isolated tributaries where there is little streamflow and little depletion. In tributaries,
604 ADF estimates of streamflow depletion tended to be greater than SVIHM and therefore ADF
605 streamflow estimates were lower than SVIHM and included more frequent drying than SVIHM.
606 However, the strong agreement in the more heavily-depleted areas means that ADFs are
607 capturing the majority of pumping impacts accurately. KGE is > 0.5 in $\sim 55\%$ of the segments for

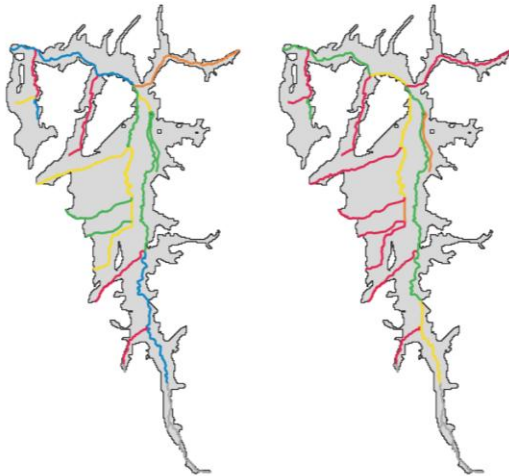
608 log(Streamflow) (Figure 8a), and these segments represent >80% of total streamflow depletion in
609 the domain (Figure 8b). Similarly, KGE is > 0.5 in ~25% of segments for streamflow depletion
610 (Figure 8a), but these represent ~70% of the total streamflow depletion in the domain (Figure
611 8b). This indicates that the impacts of pumping are best-simulated by ADFs in the settings where
612 depletion is greatest and accuracy is most important. In sum, the ADF simulations including
613 drying effectively simulate both the magnitude and spatial distribution of streamflow depletion in
614 this domain.

615

(a) log(Streamflow) (b) Streamflow Depletion
 Water Available = SVIHM No GW Irrigation scenario



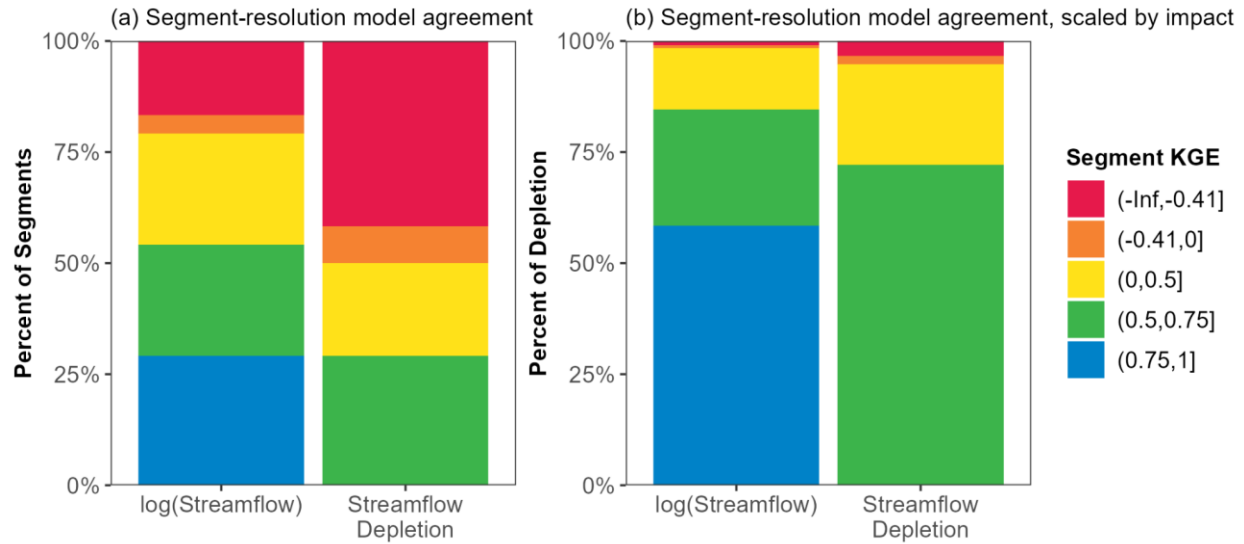
(c) log(Streamflow) (d) Streamflow Depletion
 Water Available = SVIHM No Pumping scenario



KGE — (-Inf,-0.41] — (-0.41,0] — (0,0.5] — (0.5,0.75] — (0.75,1]

616
 617
 618
 619
 620
 621
 622

Figure 7. Distribution of segment-resolution agreement between ADFs and SVIHM for (a) streamflow and (b) streamflow depletion. ADF models shown here include drying. Panels (a) and (b) use the SVIHM no groundwater irrigation scenario (#3b from Table S1) and panels (c) and (d) use the SVIHM no pumping scenario (#2 from Table S1). A KGE < -0.41 indicates that the model performs worse than using the mean of observational data (Knoben et al., 2019).



623
 624 Figure 8. Segment-resolution agreement between ADFs and SVIHM, expressed as (a) the percentage of the number
 625 of segments in the model domain and (b) the percentage of mean simulated streamflow depletion (from SVIHM)
 626 in the model domain. NA values indicate segments where a KGE could not be calculated because the ADFs did not
 627 simulate any depletion, which are the two segments at the southern inlet to Scott Valley. These results show the
 628 ADF + SVIHM + Drying model configuration with water available and SVIHM streamflow depletion calculated
 629 using the SVIHM no-pumping scenario (#2 in Table S1), as visualized in Figure 7c-d.

630

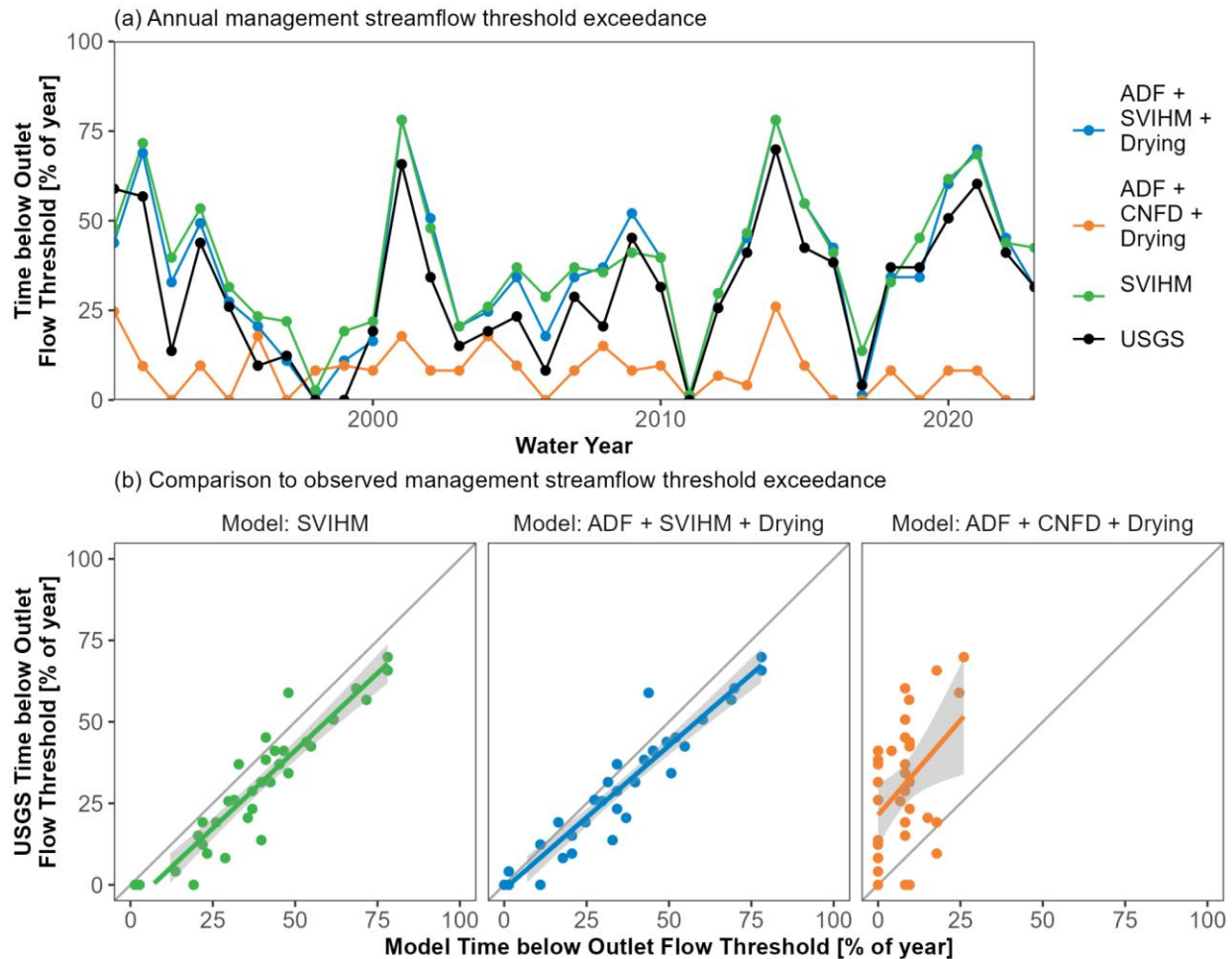
631 *4.4 Integration with water management decision-making*

632 4.4.1 Simulation of critical streamflow management thresholds

633 Accurate estimates of streamflow depletion are critical to effective integrated
 634 groundwater and surface water management. To determine if ADFs have sufficient accuracy to
 635 support local ecohydrological management decisions, we evaluated their ability to simulate the
 636 duration of streamflow below monthly minimum streamflow requirements for the gauging
 637 station at the Scott Valley watershed outlet. These streamflow thresholds are designed to provide
 638 ecological flows sufficient for salmonid survival at all life stages and vary throughout the year
 639 (Figure S8), from a minimum of 0.85 m³/sec (30 ft³/sec) in August to a maximum of 5.7 m³/sec
 640 (200 ft³/sec) in January (California State Water Resources Control Board [SWRCB], 2025). The
 641 monthly minimum streamflow requirements were developed in 2021 by the SWRCB, as
 642 recommended by the California Department of Fish and Wildlife in coordination with the
 643 National Marine Fisheries Service, and were readopted in 2022, 2024, and 2025 under additional
 644 drought emergency regulations. Under emergency drought regulations, the SWRCB has the right
 645 to curtail water users if Scott River flows fall below minimum flow requirements. As of 2025,
 646 the SWRCB is in the process of pursuing the development and implementation of permanent
 647 instream minimum flow requirements for the Scott River. As a result, the ability of streamflow
 648 depletion models to accurately estimate streamflow relative to these minimum instream flow
 649 thresholds is critical to water resources management and the future development of decision-
 650 support tools.

651 The ADF + SVIHM + Drying models simulate the annual duration of threshold
652 exceedance with comparable accuracy to the locally-calibrated SVIHM model (Figure 9). The
653 duration of model-simulated threshold exceedance agrees well with observations, with a mean
654 absolute error (MAE) of 7.3% for the ADF + SVIHM + Drying model and 9.5% for the SVIHM
655 model. In general, the models (both SVIHM and ADF + SVIHM + Drying) tend to simulate
656 slightly more threshold exceedance than was observed during dry years.

657 For basins without locally calibrated models, which are areas that ADFs can provide
658 potentially useful and low-cost estimates of streamflow and streamflow depletion, input data of
659 water available without pumping are necessary to convert depletion calculated by ADFs to
660 streamflow and, if needed, redistribute in time to account for stream drying. We tested the
661 applicability of the CNFD for this purpose and found that threshold exceedance predicted by the
662 ADF + CNFD + Drying models was positively correlated ($r = 0.42$) with the observed threshold
663 exceedance, but the percent of time exceeding the thresholds is underestimated by the ADF +
664 CNFD + Drying model (MAE = 24%; Figure 9b). This occurs because the CNFD unimpaired
665 flow estimates are higher than the SVIHM no-groundwater-irrigation scenario (Figure S5), as
666 discussed in Section 4.1. The resulting overestimates in depleted streamflow and underestimates
667 in threshold exceedance when using the CNFD could lead to inaccurate predictions of when and
668 where streamflow is below critical environmental thresholds and/or streams are dry. For
669 example, depleted streamflow in the ADF + CNFD + Drying models tends to remain above the
670 in-stream flow thresholds for most of the year, even during dry conditions like 2015 and 2021.
671 This indicates that, for decision-making processes, locally refined CNFD estimates may be
672 valuable for improving ADF model predictions (see Section 4.4.2 for additional details).



673
 674 Figure 9. (a) Number of days per year with watershed outlet streamflow below California Department of Fish and
 675 Wildlife management thresholds for each modeling approach and USGS observed flow. (b) Comparison of each
 676 modeling approach to USGS observations. ADF simulations plotted here include drying.
 677

678 4.4.2 Transferability to other settings

679 Scott Valley was an ideal setting to develop and test the methods developed in this study
 680 due to the highly transmissive aquifer that is well-connected to the stream, the availability of
 681 high-quality input datasets developed as part of the creation of SVIHM, and the presence of both
 682 SVIHM simulations and streamflow observations for evaluation. The potential applicability of
 683 ADFs in other watersheds would be dependent on the suitability of analytical models for those
 684 settings. For example, ADFs would not be expected to work well in settings where the water
 685 table is disconnected from the stream (e.g., by a confining layer) since ADFs assume a
 686 connection between the groundwater being pumped and the surface water network. Additionally,
 687 settings with a highly heterogeneous subsurface, such as where fracture flow dominates stream-
 688 aquifer interactions, may not be well-simulated by ADFs since the simplifying assumptions in
 689 analytical models are violated. These types of hydrogeologic settings are also notoriously hard to
 690 simulate with numerical models and an area where additional method development is needed.

691 However, where the subsurface is heterogeneous but groundwater flow is still through porous
692 media, it is possible to incorporate some heterogeneity into ADFs by integrating multiple
693 geological units into calculations of effective transmissivity and storativity (as described in
694 Appendix A of Li et al., 2022) and defining different hydrostratigraphic parameters separately
695 for each well-stream pair to account for spatial differences in subsurface properties. This
696 averaging process, however, inherently will reduce the ability of ADFs to represent spatial
697 heterogeneity of responses to pumping and lead to uncertainty in model output.

698 ADFs are also applicable only where there is sufficient input data. Groundwater pumping
699 locations, rates, and schedules are critical inputs to both analytical and numerical models, but
700 water use data are unavailable in many settings (Marston et al., 2022). Flowmeters on pumping
701 wells are the most accurate approach to developing water use input datasets, but these data are
702 rarely collected or publicly available (Foster et al., 2020). Remote sensing approaches may be a
703 potentially valuable tool for estimating field-resolution water use (Ott et al., 2024; Zipper et al.,
704 2024, Jalilvand et al., 2023), though these approaches can struggle to identify changes in
705 irrigation efficiency when consumptive use does not change (Asarian et al., 2025). Other
706 approaches to estimate groundwater use include interpretation of groundwater hydrographs
707 (Brookfield et al., 2024) and the application of crop models (Lamsal & Marston, 2025). The
708 SVIHM estimates water using process-based simulations of crop water requirements to estimate
709 local water needs, and partitions these between surface water and groundwater sources (Tolley et
710 al., 2019). Since water use is a primary control over the volume of streamflow depletion,
711 continued refinement of techniques for estimating the timing and location of groundwater
712 withdrawals is critical to improving analytical, numerical, or statistical models of streamflow
713 depletion.

714 For incorporation of stream drying into ADFs, estimates of segment-resolution water
715 available (i.e., the $WA_{k,t}$ term described in Section 3.4.2) are required. In settings that do not have
716 locally-calibrated streamflow models, there are multiple approaches that could be explored to
717 develop reliable water available estimates. In California, regional statistical models like CNFD
718 are available, and in other domains there is an increasing abundance of data-driven models that
719 could provide local non-depleted streamflow estimates (Kratzert et al., 2019, 2022). Since data-
720 driven modeling, to date, has primarily focused on reference watersheds with relatively minor
721 human impacts, predictions from these models for ungauged basins may be representative of
722 non-depleted streamflow. However, these data-driven modeling efforts primary focus on
723 watershed-scale predictions, rather than providing segment-resolution data that is needed for
724 incorporation into ADFs. There are also an increasing number of regional- to national-scale
725 process-based models, such as the National Hydrologic Model (NHM; Regan et al., 2019) or
726 ParFlow-CONUS (Condon & Maxwell, 2019; Maxwell et al., 2015), which simulate streamflow
727 at the resolution of individual stream segments based on governing physical equations. Since
728 many national-scale models do not explicitly incorporate groundwater pumping (Bosompemaa et
729 al., 2025; Towler et al., 2023), or can be run in both pumping-on and pumping-off configurations
730 (Condon & Maxwell, 2019), their flow estimates could provide a useful segment-resolution
731 water available input for the ADF models.

732 Beyond input data needs, incorporating a local calibration and bias correction approach
733 into ADF workflows would likely improve transferability and better match observed streamflow.
734 The ADFs used in this study are not calibrated, though they use calibrated model parameters
735 from SVIHM as inputs. In most settings, hydrostratigraphic inputs (such as transmissivity and
736 storativity) and ADF-specific parameters (such as the weighting factor for depletion
737 apportionment) will need to be estimated and refined based on local data. Developing
738 appropriate parameter estimates can add time and expense to the model development process, but
739 could decrease model uncertainty by better constraining ADF inputs. The primary ADF
740 uncertainty addressed in this study is the result of different water available input datasets,
741 through our comparison of CNFD and multiple SVIHM scenarios (in Table S1), and we find that
742 selection of an appropriate water available data source is essential to developing accurate
743 estimates of depleted streamflow and stream drying. For use in settings without well-known
744 input data, ADF model parameters and inputs (including water available) could be calibrated to
745 improve agreement with observed streamflow data, as is typically done for numerical models of
746 streamflow depletion (Barlow et al., 2018; Fienen et al., 2018; Foster et al., 2021). This process
747 would provide an opportunity for calculating robust uncertainty estimates, which are critical to
748 effective decision-support modeling efforts (Doherty & Moore, 2020) and enhance user
749 confidence in model outputs (Afzal et al., 2025). There are existing open-source tools for
750 parameter estimation and uncertainty analysis that are well-suited for integration with ADFs
751 (Ford et al., 2024; White et al., 2021).

752 For ungauged areas where no streamflow data are available for calibration, additional
753 work would be needed to identify locally-appropriate refinements. One potential pathway for this
754 could be parameter regionalization, in which calibrated parameters are developed for locations
755 where outputs can be compared to observations, and then these parameters are transferred to
756 other settings with similar hydrological characteristics (Bawa et al., 2025; Beck et al., 2016;
757 Mihret et al., 2025). Future work evaluating the feasibility of this approach, and resulting
758 uncertainties, would be valuable to better understand the potential for transferability to other
759 domains.

760 4.4.3 Integrating multiple modeling approaches to meet management needs

761 Streamflow depletion cannot be measured directly at the scales relevant to regional water
762 resource management, and therefore modeling tools must be developed to support decision-
763 making (Zipper et al., 2024). While a globally relevant issue, this technical need has recently
764 emerged within two management contexts in California. As previously mentioned, assessing
765 depletion of interconnected surface waters is a requirement under SGMA, and many
766 groundwater managers across the state must develop models capable of estimating streamflow
767 depletion. Additionally, courts in California have recently ruled that groundwater withdrawals
768 are subject to regulation under the Public Trust Doctrine on the basis that groundwater
769 withdrawals have the potential to harm navigable waterways (*Environmental Law Foundation v.*
770 *State Water Resources Control Board*, 2018). This has resulted in county agency efforts to revise
771 well permitting regulations and has highlighted the need for modeling tools to estimate potential

772 impacts of streamflow depletion on public trust resources such as navigable waters or aquatic
773 ecosystems.

774 In many management contexts, it is likely that a combination of analytical and numerical
775 methods will be implemented as groundwater managers balance resource constraints (time, cost,
776 available technical expertise, risk of significant impacts, etc., as discussed in Zipper et al.,
777 2022a). Our analysis demonstrates that ADFs may be implemented effectively as low-
778 complexity, low-cost techniques in hydrogeologic settings where their simplifying assumptions
779 hold (i.e. alluvial groundwater subbasins where a high degree of interconnectivity between
780 surface and groundwater resources exist) and ADFs can be accurately extended outside these
781 conditions where reasonable process-representations can be developed, as we demonstrate with
782 our simplified approach for stream drying (Figure 1b). For example, remote sensing tools could
783 provide an opportunity to estimate consumptive water use by agriculture, which could be used to
784 account for potential changes in the water balance associated with changes in pumping such as
785 irrigation return flows (Asarian et al., 2025). This emerging ADF modeling framework is
786 promising based upon its ability to be developed as a cost-effective solution to estimating
787 streamflow depletion due to groundwater pumping and potential integration into web-based
788 decision support tools (Huggins et al., 2018). Numerical models will continue to be key tools in
789 complex settings where water resources management decision-making benefits from a detailed
790 representation of water balance dynamics or necessitates complex management scenario
791 simulations (managed aquifer recharge, phreatophytic evapotranspiration dynamics, reservoir
792 operations, etc.). Importantly, pumping changes are often associated with changes to land use
793 and impact other hydrological fluxes including recharge, evapotranspiration, and runoff. To
794 avoid unintended consequences, effective water management strategies must account for the
795 holistic impacts of pumping decisions on the water balance. A unified modeling philosophy that
796 utilizes a suite of streamflow depletion modeling methods in varying contexts and considers
797 integrated impacts of land use and water management changes simultaneously will provide
798 groundwater managers with the flexibility to develop decision-support tools appropriate to the
799 scope of their specific needs.

800

801 **5. Conclusions**

802 Analytical depletion functions (ADFs) are a low-complexity and scalable approach that
803 provide accurate estimates of both streamflow and streamflow depletion for the Scott River
804 Valley. This work describes pumping-induced stream drying and resulting lagged pumping
805 impacts on streamflow, where disconnection during drying delays streamflow depletion until the
806 seasonal rewetting period, and provides a mechanistic, water-budget-based framework for
807 simulating these processes. We find that ADF estimates of streamflow are comparable to
808 observed streamflow from a USGS gauging station at the watershed outlet ($KGE = 0.91$, $R^2 =$
809 0.92 , normalized RMSE = 5.9%) and consistent with simulated streamflow by SVIHM, a
810 process-based integrated hydrologic model developed for the watershed. ADFs also accurately
811 predict how frequently streamflow drops below critical management thresholds (MAE = 7.3%).

812 However, developing accurate estimates of streamflow and streamflow depletion using ADFs
813 requires a locally accurate estimate of non-depleted streamflow (what streamflow would have
814 been without groundwater pumping). ADFs simulate the direct effects of pumping on
815 streamflow, and do not explicitly account for other changes in the water balance caused by the
816 conversion of natural vegetation to irrigated agriculture, and therefore could be enhanced by
817 integration with estimates of other water balance changes associated with pumping practices, for
818 example remotely sensed estimates of differences in consumptive water use. We show that using
819 a regional statistical model, the California Natural Flows Database (CNFD), provided reasonable
820 temporal dynamics, but estimated non-depleted streamflow by CNFD is higher than the non-
821 depleted streamflow simulated by SVIHM. As a result, ADFs using CNFD as an input
822 overestimate streamflow. This suggests that developing an approach to locally calibrate and
823 refine ADFs using CNFD may have potential for streamflow depletion assessments in ungauged
824 and unmodeled watersheds. For integration into decision-support applications, future work
825 should also include explicit quantification of uncertainty associated with different structural and
826 parametric components of ADF estimates to ensure reliability.

827 Incorporating stream drying, and associated temporal redistribution of streamflow
828 depletion, is critical to accurately estimate streamflow and streamflow depletion in this domain at
829 sub-annual scales. We demonstrate that reductions in hydrologic connectivity caused by stream
830 drying can lead to substantial lags in the manifestation of streamflow depletion. These lags occur
831 because, when the streams dry, continued pumping leads to increased groundwater depletion as
832 the stream and aquifer are disconnected. When the hydrologic system rewets in the fall/winter
833 rainy season, there are greater stream losses due to increased infiltration through the streambed
834 until the depleted groundwater system is replenished and the stream-aquifer system is
835 reconnected. We incorporate this process into ADF models using a simple water budget
836 approach at the stream reach resolution and route the resulting changes in the timing of
837 streamflow downstream through the river network. This representation of stream drying shows
838 strong agreement with both SVIHM and observed streamflow and advance ADFs towards
839 potential application as a water management decision-support tool.

840 **Acknowledgments**

841 We appreciate useful feedback from Ben Kerr, Laura Foglia, Matt O'Connor, Jeremy Kobor, and
842 two anonymous reviewers.

843 **Data and Code Availability**

844 ADFs are available in the streamDepletr package for R: [https://cran.r-
845 project.org/package=streamDepletr](https://cran.r-project.org/package=streamDepletr)

846 SVIHM is available at: <https://github.com/UCDavisHydro/SVIHM>

847 The data and code used in this study are available on HydroShare:

848 <http://www.hydroshare.org/resource/f36f9b62549c46498bba89db66a8cbc5>

849 **Funding**

850 This work was supported by The Nature Conservancy grants #10192023-16680 and #06132024-
851 17291 to SZ.

852 **Declaration of interests**

853 The authors have nothing to declare.

854 **Declaration of generative AI and AI-assisted technologies in the writing process**

855 During the preparation of this work the lead author used ChatGPT in order to explore alternate
856 programming approaches to create directed stream network graphs and incorporate stream
857 drying, which were then tested by the author for suitability and efficiency. After using this
858 tool/service, the author reviewed and edited the content as needed and take full responsibility for
859 the content of the published article.

860 **Author contributions**

861 SZ: Conceptualization, Data curation, Formal Analysis, Funding acquisition, Investigation,
862 Methodology, Project administration, Software, Supervision, Validation, Visualization, Writing
863 – original draft, Writing – review & editing

864

865 IG: Data curation, Formal Analysis, Investigation, Methodology, Software, Visualization,
866 Writing – review & editing

867

868 NM: Conceptualization, Data curation, Funding acquisition, Investigation, Methodology, Project
869 administration, Writing – original draft, Writing – review & editing

870

871 MS: Conceptualization, Funding acquisition, Methodology, Project administration, Writing –
872 review & editing

873

874 CK: Data curation, Methodology, Investigation, Software, Validation, Writing – review &
875 editing

876

877 LS: Data curation, Methodology, Investigation, Software, Validation, Writing – original draft,
878 Writing – review & editing

879

880 TH: Funding acquisition, Methodology, Supervision, Writing – review & editing

881

882 **References**

883 Abimbola, O. P., Mittelstet, A. R., & Gilmore, T. E. (2020a). Geostatistical features of streambed
884 vertical hydraulic conductivities in Frenchman Creek Watershed in Western Nebraska.

885 *Hydrological Processes*, 34(16), 3481–3491. <https://doi.org/10.1002/hyp.13823>

886 Abimbola, O. P., Mittelstet, A. R., Gilmore, T. E., & Korus, J. T. (2020b). Influence of
887 watershed characteristics on streambed hydraulic conductivity across multiple stream
888 orders. *Scientific Reports*, 10(1), 3696. <https://doi.org/10.1038/s41598-020-60658-3>

889 Afzal, N., Swenson, L.J., Zipper, S., Zwickle, A., & Wardropper, C.B. (2025). Using values-

890 informed mental models to understand farmer, water manager, and scientist use and
891 perceptions of hydrologic models. *Journal of Hydrology*, 658, 133171.
892 <https://doi.org/10.1016/j.jhydrol.2025.133171>

893 Asarian, J.E., Stanford, B., Murphy, N.P., & Pollock, M.M. (2025). Pairing OpenET remotely
894 sensed evapotranspiration with streamflow data to assess the effectiveness of irrigation
895 curtailment for aquatic conservation. *Journal of Hydrology*, 663, 134119.
896 <https://doi.org/10.1016/j.jhydrol.2025.134119>

897 Barlow, P. M., Leake, S. A., & Fienen, M. N. (2018). Capture Versus Capture Zones: Clarifying
898 Terminology Related to Sources of Water to Wells. *Groundwater*, 56(5), 694–704.
899 <https://doi.org/10.1111/gwat.12661>

900 Barlow, P. M., & Leake, S. A. (2012). *Streamflow depletion by wells--Understanding and*
901 *managing the effects of groundwater pumping on streamflow* (No. Circular 1376). Reston
902 VA: U.S. Geological Survey. Retrieved from <https://pubs.usgs.gov/circ/1376/>

903 Bawa, A., Mendoza, K., Srinivasan, R., O'Donchha, F., Smith, D., Wolfe, K., Parmar, R.,
904 Johnston, J. M., & Corona, J. (2025). Enhancing hydrological modeling of ungauged
905 watersheds through machine learning and physical similarity-based regionalization of
906 calibration parameters. *Environmental Modelling & Software*, 186, 106335.
907 <https://doi.org/10.1016/j.envsoft.2025.106335>

908 Beck, H. E., van Dijk, A. I. J. M., de Roo, A., Miralles, D. G., McVicar, T. R., Schellekens, J., &
909 Bruijnzeel, L. A. (2016). Global-scale regionalization of hydrologic model parameters.
910 *Water Resources Research*, 52(5), 3599–3622. <https://doi.org/10.1002/2015WR018247>

911 Bosompemaa, P., Brookfield, A., Zipper, S., & Hill, M. C. (2025). Using national hydrologic
912 models to obtain regional climate change impacts on streamflow basins with
913 unrepresented processes. *Environmental Modelling & Software*, 183, 106234.
914 <https://doi.org/10.1016/j.envsoft.2024.106234>

915 Brookfield, A.E., Zipper, S., Kendall, A.D., Ajami, H., & Deines, J.M. (2024). Estimating
916 Groundwater Pumping for Irrigation: A Method Comparison. *Groundwater*, 62, 15–33.
917 <https://doi.org/10.1111/gwat.13336>

918 California Department of Water Resources. (2024). *Depletion of Interconnected Surface Water:*
919 *An Introduction*. Retrieved from [https://data.cnra.ca.gov/dataset/68e0d8b6-a207-4b30-](https://data.cnra.ca.gov/dataset/68e0d8b6-a207-4b30-a16b-3daeb659faea/resource/218e3361-c142-400f-a97f-5dfa79cd4997/download/depletionsofisw_paper1_intro_draft.pdf)
920 [a16b-3daeb659faea/resource/218e3361-c142-400f-a97f-](https://data.cnra.ca.gov/dataset/68e0d8b6-a207-4b30-a16b-3daeb659faea/resource/218e3361-c142-400f-a97f-5dfa79cd4997/download/depletionsofisw_paper1_intro_draft.pdf)
921 [5dfa79cd4997/download/depletionsofisw_paper1_intro_draft.pdf](https://data.cnra.ca.gov/dataset/68e0d8b6-a207-4b30-a16b-3daeb659faea/resource/218e3361-c142-400f-a97f-5dfa79cd4997/download/depletionsofisw_paper1_intro_draft.pdf)

922 California State Water Resources Control Board. (2025). *Finding of Emergency and Informative*
923 *Digest: Proposed Scott River and Shasta River Watersheds Emergency Regulation*.
924 Sacramento CA: California State Water Resources Control Board. Retrieved from
925 [https://www.waterboards.ca.gov/drought/scott_shasta_rivers/docs/2025/scott-shasta-](https://www.waterboards.ca.gov/drought/scott_shasta_rivers/docs/2025/scott-shasta-drought-informative-digest.pdf)
926 [drought-informative-digest.pdf](https://www.waterboards.ca.gov/drought/scott_shasta_rivers/docs/2025/scott-shasta-drought-informative-digest.pdf)

927 Christensen, S. (2000). On the Estimation of Stream Flow Depletion Parameters by Drawdown
928 Analysis. *Groundwater*, 38(5), 726–734. [https://doi.org/10.1111/j.1745-](https://doi.org/10.1111/j.1745-6584.2000.tb02708.x)
929 [6584.2000.tb02708.x](https://doi.org/10.1111/j.1745-6584.2000.tb02708.x)

930 Condon, L. E., & Maxwell, R. M. (2019). Simulating the sensitivity of evapotranspiration and
931 streamflow to large-scale groundwater depletion. *Science Advances*, 5(6), eaav4574.
932 <https://doi.org/10.1126/sciadv.aav4574>

933 Datry, T., Truchy, A., Olden, J. D., Busch, M. H., Stubbington, R., Dodds, W. K., Zipper, S., Yu,
934 S., Messenger, M. L., Tonkin, J. D., Kaiser, K. E., Hammond, J. C., Moody, E. K.,
935 Burrows, R. M., Sarremejane, R., DelVecchia, A. G., Fork, M. L., Little, C. J., ... Allen,

936 D. (2022). Causes, Responses, and Implications of Anthropogenic versus Natural Flow
937 Intermittence in River Networks. *BioScience*, biac098.
938 <https://doi.org/10.1093/biosci/biac098>

939 Doherty, J. & Moore, C. (2020). Decision Support Modeling: Data Assimilation, Uncertainty
940 Quantification, and Strategic Abstraction. *Groundwater*, 58, 327–337.
941 <https://doi.org/10.1111/gwat.12969>

942 Environmental Law Foundation v. State Water Resources Control Board, 26 Cal.App.5th 844
943 Cal. Rptr. 3d 393 237 (Cal. Ct. App. 2018).

944 Falke, J. A., Fausch, K. D., Magelky, R., Aldred, A., Durnford, D. S., Riley, L. K., & Oad, R.
945 (2011). The role of groundwater pumping and drought in shaping ecological futures for
946 stream fishes in a dryland river basin of the western Great Plains, USA. *Ecohydrology*,
947 4(5), 682–697. <https://doi.org/10.1002/eco.158>

948 Fienen, M. N., Bradbury, K. R., Kniffin, M., & Barlow, P. M. (2018). Depletion Mapping and
949 Constrained Optimization to Support Managing Groundwater Extraction. *Groundwater*,
950 56(1), 18–31. <https://doi.org/10.1111/gwat.12536>

951 Flores, L., Bailey, R. T., & Kraeger-Rovey, C. (2020). Analyzing the Effects of Groundwater
952 Pumping on an Urban Stream-Aquifer System. *JAWRA Journal of the American Water*
953 *Resources Association*, 56(2), 310–322. <https://doi.org/10.1111/1752-1688.12827>

954 Foglia, L., McNally, A., & Harter, T. (2013). Coupling a spatiotemporally distributed soil water
955 budget with stream-depletion functions to inform stakeholder-driven management of
956 groundwater-dependent ecosystems. *Water Resources Research*, 49(11), 7292–7310.
957 <https://doi.org/10.1002/wrcr.20555>

958 Foglia, L., Neumann, J., Tolley, D., Orloff, S., Snyder, R., & Harter, T. (2018). Modeling guides
959 groundwater management in a basin with river–aquifer interactions. *California*
960 *Agriculture*, 72(1), 84–95.

961 Ford, C., Ha, W., Markovich, K., & Zwinger, J. (2024). Jupyter Notebooks for Parameter
962 Estimation, Uncertainty Analysis, and Optimization with PEST++. *Groundwater*, 62,
963 825–829. <https://doi.org/10.1111/gwat.13447>

964 Foster, L. K., White, J. T., Leaf, A. T., Houston, N. A., & Teague, A. (2021). Risk-Based
965 Decision-Support Groundwater Modeling for the Lower San Antonio River Basin, Texas,
966 USA. *Groundwater*, 59(4), 581–596. <https://doi.org/10.1111/gwat.13107>

967 Foster, T., Mieno, T., & Brozović, N. (2020). Satellite-Based Monitoring of Irrigation Water
968 Use: Assessing Measurement Errors and Their Implications for Agricultural Water
969 Management Policy. *Water Resources Research*, 56, e2020WR028378.
970 <https://doi.org/10.1029/2020WR028378>

971 Gage, A., & Milman, A. (2020). Groundwater Plans in the United States: Regulatory
972 Frameworks and Management Goals. *Groundwater*. <https://doi.org/10.1111/gwat.13050>

973 Glover, R. E., & Balmer, G. G. (1954). River depletion resulting from pumping a well near a
974 river. *Eos, Transactions American Geophysical Union*, 35(3), 468–470.
975 <https://doi.org/10.1029/TR035i003p00468>

976 Grantham, T. E., Carlisle, D. M., Howard, J., Lane, B., Lusardi, R., Obester, A., Sandoval-Solis,
977 S., Stanford, B., Stein, E. D., Taniguchi-Quan, K. T., Yarnell, S. M., & Zimmerman, J. K.
978 H. (2022). Modeling Functional Flows in California’s Rivers. *Frontiers in Environmental*
979 *Science*, 10. <https://doi.org/10.3389/fenvs.2022.787473>

980 Gupta, H. V., Kling, H., Yilmaz, K. K., & Martinez, G. F. (2009). Decomposition of the mean
981 squared error and NSE performance criteria: Implications for improving hydrological

- 982 modelling. *Journal of Hydrology*, 377(1), 80–91.
983 <https://doi.org/10.1016/j.jhydrol.2009.08.003>
- 984 Hammond, J. C., Zimmer, M., Shanafield, M., Kaiser, K., Godsey, S. E., Mims, M. C., Zipper, S.
985 C., Burrows, R. M., Kampf, S. K., Dodds, W., Jones, C. N., Krabbenhoft, C. A.,
986 Boersma, K. S., Datry, T., Olden, J. D., Allen, G. H., Price, A. N., Costigan, K., ... Allen,
987 D. C. (2021). Spatial Patterns and Drivers of Nonperennial Flow Regimes in the
988 Contiguous United States. *Geophysical Research Letters*, 48(2), e2020GL090794.
989 <https://doi.org/10.1029/2020GL090794>
- 990 Hantush, M. S. (1965). Wells near streams with semipervious beds. *Journal of Geophysical*
991 *Research*, 70(12), 2829–2838. <https://doi.org/10.1029/JZ070i012p02829>
- 992 Harter, T. (2020). California’s 2014 Sustainable Groundwater Management Act – From the Back
993 Seat to the Driver Seat in the (Inter)National Groundwater Sustainability Movement. In
994 J.-D. Rinaudo, C. Holley, S. Barnett, & M. Montginoul (Eds.), *Sustainable Groundwater*
995 *Management: A Comparative Analysis of French and Australian Policies and*
996 *Implications to Other Countries* (pp. 511–536). Cham: Springer International Publishing.
997 https://doi.org/10.1007/978-3-030-32766-8_26
- 998 Huang, C.-S., Yang, T., & Yeh, H.-D. (2018). Review of analytical models to stream depletion
999 induced by pumping: Guide to model selection. *Journal of Hydrology*, 561, 277–285.
1000 <https://doi.org/10.1016/j.jhydrol.2018.04.015>
- 1001 Huggins, X., Gleeson, T., Eckstrand, H., & Kerr, B. (2018). Streamflow Depletion Modeling:
1002 Methods for an Adaptable and Conjunctive Water Management Decision Support Tool.
1003 *JAWRA Journal of the American Water Resources Association*, 54(5), 1024–1038.
1004 <https://doi.org/10.1111/1752-1688.12659>
- 1005 Hunt, B. (1999). Unsteady Stream Depletion from Ground Water Pumping. *Ground Water*,
1006 37(1), 98–102. <https://doi.org/10.1111/j.1745-6584.1999.tb00962.x>
- 1007 Hunt, B., Weir, J., & Clausen, B. (2001). A Stream Depletion Field Experiment. *Ground Water*,
1008 39(2), 283–289. <https://doi.org/10.1111/j.1745-6584.2001.tb02310.x>
- 1009 Jalilvand, E., Abolafia-Rosenzweig, R., Tajrishy, M., Kumar, S.V., Mohammadi, M.R. & Das,
1010 N.N. (2023). Is It Possible to Quantify Irrigation Water-Use by Assimilating a High-
1011 Resolution Satellite Soil Moisture Product? *Water Resources Research* 59,
1012 e2022WR033342. <https://doi.org/10.1029/2022WR033342>
- 1013 Kallis, G., & Butler, D. (2001). The EU water framework directive: measures and implications.
1014 *Water Policy*, 3(2), 125–142. [https://doi.org/10.1016/S1366-7017\(01\)00007-1](https://doi.org/10.1016/S1366-7017(01)00007-1)
- 1015 Knoben, W. J. M., Freer, J. E., & Woods, R. A. (2019). Technical note: Inherent benchmark or
1016 not? Comparing Nash–Sutcliffe and Kling–Gupta efficiency scores. *Hydrology and Earth*
1017 *System Sciences*, 23(10), 4323–4331. <https://doi.org/10.5194/hess-23-4323-2019>
- 1018 Kollet, S. J., & Zlotnik, V. A. (2003). Stream depletion predictions using pumping test data from
1019 a heterogeneous stream–aquifer system (a case study from the Great Plains, USA).
1020 *Journal of Hydrology*, 281(1), 96–114. [https://doi.org/10.1016/S0022-1694\(03\)00203-8](https://doi.org/10.1016/S0022-1694(03)00203-8)
- 1021 Korus, J. T., Fraundorfer, W. P., Gilmore, T. E., & Karnik, K. (2020). Transient streambed
1022 hydraulic conductivity in channel and bar environments, Loup River, Nebraska.
1023 *Hydrological Processes*, 34(14), 3061–3077. <https://doi.org/10.1002/hyp.13777>
- 1024 Korus, J. T., Gilmore, T. E., Waszgis, M. M., & Mittelstet, A. R. (2018). Unit-bar migration and
1025 bar-trough deposition: impacts on hydraulic conductivity and grain size heterogeneity in
1026 a sandy streambed. *Hydrogeology Journal*, 26(2), 553–564.
1027 <https://doi.org/10.1007/s10040-017-1661-6>

- 1028 Kouba, C., & Harter, T. (2024). Seasonal prediction of end-of-dry-season watershed behavior in
 1029 a highly interconnected alluvial watershed in northern California. *Hydrology and Earth*
 1030 *System Sciences*, 28(3), 691–718. <https://doi.org/10.5194/hess-28-691-2024>
- 1031 Kratzert, F., Nearing, G., Addor, N., Erickson, T., Gauch, M., Gilon, O., Gudmundsson, L.,
 1032 Hassidim, A., Klotz, D., Nevo, S., Shalev, G., & Matias, Y. (2022). Caravan - A global
 1033 community dataset for large-sample hydrology. Retrieved from
 1034 <https://eartharxiv.org/repository/view/3345/>
- 1035 Kratzert, F., Klotz, D., Herrnegger, M., Sampson, A. K., Hochreiter, S., & Nearing, G. S. (2019).
 1036 Toward Improved Predictions in Ungauged Basins: Exploiting the Power of Machine
 1037 Learning. *Water Resources Research*, 55(12), 11344–11354.
 1038 <https://doi.org/10.1029/2019WR026065>
- 1039 Lamsal, G. & Marston, L.T. (2025). Monthly Crop Water Consumption of Irrigated Crops in the
 1040 United States From 1981 to 2019. *Water Resources Research*, 61, e2024WR038334.
 1041 <https://doi.org/10.1029/2024WR038334>
- 1042 Lapides, D., Maitland, B. M., Zipper, S. C., Latzka, A. W., Pruitt, A., & Greve, R. (2022).
 1043 Advancing environmental flows approaches to streamflow depletion management.
 1044 *Journal of Hydrology*, 127447. <https://doi.org/10.1016/j.jhydrol.2022.127447>
- 1045 Leahy, T. (2016). Desperate Times Call for Sensible Measures: The Making of the California
 1046 Sustainable Groundwater Management Act. *Golden Gate University Environmental Law*
 1047 *Journal*, 9(1), 5.
- 1048 Li, Q., Zipper, S. C., & Gleeson, T. (2020). Streamflow depletion from groundwater pumping in
 1049 contrasting hydrogeological landscapes: Evaluation and sensitivity of a new management
 1050 tool. *Journal of Hydrology*, 590, 125568. <https://doi.org/10.1016/j.jhydrol.2020.125568>
- 1051 Li, Q., Gleeson, T., Zipper, S. C., & Kerr, B. (2022). Too Many Streams and Not Enough Time
 1052 or Money? Analytical Depletion Functions for Streamflow Depletion Estimates.
 1053 *Groundwater*, 60(1), 145–155. <https://doi.org/10.1111/gwat.13124>
- 1054 Mack, S. (1958). *Geology and ground-water features of Scott Valley, Siskiyou County,*
 1055 *California* (No. Water Supply Paper 1462). *Water Supply Paper* (p. 98). U.S. Govt. Print.
 1056 Off., <https://doi.org/10.3133/wsp1462>
- 1057 Malama, B., Lin, Y.-F., & Kuhlman, K. L. (2024). Semi-Analytical Modeling of Transient
 1058 Stream Drawdown and Depletion in Response to Aquifer Pumping. *Groundwater*, 62(6),
 1059 904–919. <https://doi.org/10.1111/gwat.13425>
- 1060 Marston, L.T., Abdallah, A.M., Bagstad, K.J., Dickson, K., Glynn, P., Larsen, S.G., Melton,
 1061 F.S., Onda, K., Painter, J.A., Prairie, J., Ruddell, B.L., Rushforth, R.R., Senay, G.B. &
 1062 Shaffer, K. (2022). Water-Use Data in the United States: Challenges and Future
 1063 Directions. *JAWRA Journal of the American Water Resources Association*, 58, 485–495.
 1064 <https://doi.org/10.1111/1752-1688.13004>
- 1065 Maxwell, R. M., Condon, L. E., & Kollet, S. J. (2015). A high-resolution simulation of
 1066 groundwater and surface water over most of the continental US with the integrated
 1067 hydrologic model ParFlow v3. *Geoscientific Model Development*, 8(3), 923–937.
 1068 <https://doi.org/10.5194/gmd-8-923-2015>
- 1069 Messenger, M. L., Lehner, B., Cockburn, C., Lamouroux, N., Pella, H., Snelder, T., Tockner, K.,
 1070 Trautmann, T., Watt, C., & Datry, T. (2021). Global prevalence of non-perennial rivers
 1071 and streams. *Nature*, 594(7863), 391–397. <https://doi.org/10.1038/s41586-021-03565-5>
- 1072 Mihret, T. T., Zemale, F. A., Worqlul, A. W., Ayalew, A. D., & Fohrer, N. (2025). Unlocking
 1073 watershed mysteries: Innovative regionalization of hydrological model parameters in

1074 data-scarce regions. *Journal of Hydrology: Regional Studies*, 57, 102163.
1075 <https://doi.org/10.1016/j.ejrh.2024.102163>

1076 Nyholm, T., Christensen, S., & Rasmussen, K. R. (2002). Flow Depletion in a Small Stream
1077 Caused by Ground Water Abstraction from Wells. *Ground Water*, 40(4), 425–437.
1078 <https://doi.org/10.1111/j.1745-6584.2002.tb02521.x>

1079 Ott, T.J., Majumdar, S., Huntington, J.L., Pearson, C., Bromley, M., Minor, B.A., ReVelle, P.,
1080 Morton, C.G., Sueki, S., Beamer, J.P. & Jasoni, R.L. (2024). Toward field-scale
1081 groundwater pumping and improved groundwater management using remote sensing and
1082 climate data. *Agricultural Water Management*, 302, 109000.
1083 <https://doi.org/10.1016/j.agwat.2024.109000>

1084 Owen, D., Cantor, A., Nylen, N. G., Harter, T., & Kiparsky, M. (2019). California groundwater
1085 management, science-policy interfaces, and the legacies of artificial legal distinctions.
1086 *Environmental Research Letters*, 14(4), 045016. [https://doi.org/10.1088/1748-](https://doi.org/10.1088/1748-9326/ab0751)
1087 [9326/ab0751](https://doi.org/10.1088/1748-9326/ab0751)

1088 Price, A. N., Zimmer, M. A., Bergstrom, A., Burgin, A. J., Seybold, E. C., Krabbenhoft, C. A.,
1089 Zipper, S., Busch, M. H., Dodds, W. K., Walters, A., Rogosch, J. S., Stubbington, R.,
1090 Walker, R. H., Stegen, J. C., Datry, T., Messenger, M., Olden, J., Godsey, S. E., ... Ward,
1091 A. (2024). Biogeochemical and community ecology responses to the wetting of non-
1092 perennial streams. *Nature Water*, 2(9), 815–826. [https://doi.org/10.1038/s44221-024-](https://doi.org/10.1038/s44221-024-00298-3)
1093 [00298-3](https://doi.org/10.1038/s44221-024-00298-3)

1094 Price, A. N., Jones, C. N., Hammond, J. C., Zimmer, M. A., & Zipper, S. C. (2021). The Drying
1095 Regimes of Non-Perennial Rivers and Streams. *Geophysical Research Letters*, 48(14),
1096 e2021GL093298. <https://doi.org/10.1029/2021GL093298>

1097 Reeves, H. W., Hamilton, D. A., Seelbach, P. W., & Asher, A. J. (2009). *Ground-water-*
1098 *withdrawal component of the Michigan water-withdrawal screening tool* (Scientific
1099 Investigations Report No. 2009–5003) (p. 36). Reston VA: U.S. Geological Survey.
1100 Retrieved from <https://pubs.usgs.gov/sir/2009/5003/>

1101 Regan, R. S., Juracek, K. E., Hay, L. E., Markstrom, S. L., Viger, R. J., Driscoll, J. M.,
1102 LaFontaine, J. H., & Norton, P. A. (2019). The U. S. Geological Survey National
1103 Hydrologic Model infrastructure: Rationale, description, and application of a watershed-
1104 scale model for the conterminous United States. *Environmental Modelling & Software*,
1105 111, 192–203. <https://doi.org/10.1016/j.envsoft.2018.09.023>

1106 Rohde, M. M., Freund, R., & Howard, J. (2017). A Global Synthesis of Managing Groundwater
1107 Dependent Ecosystems Under Sustainable Groundwater Policy. *Groundwater*, 55(3),
1108 293–301. <https://doi.org/10.1111/gwat.12511>

1109 Ross, A. (2018). Speeding the transition towards integrated groundwater and surface water
1110 management in Australia. *Journal of Hydrology*, 567, e1–e10.
1111 <https://doi.org/10.1016/j.jhydrol.2017.01.037>

1112 RRCA. (2003). *Republican River Compact Administration Ground Water Model*. Republican
1113 River Compact Administration. Retrieved from <http://www.republicanrivercompact.org/>

1114 Sauquet, E., Shanafield, M., Hammond, J., Sefton, C., Leigh, C., & Datry, T. (2021).
1115 Classification and trends in intermittent river flow regimes in Australia, northwestern
1116 Europe and USA: a global perspective. *Journal of Hydrology*, 126170.
1117 <https://doi.org/10.1016/j.jhydrol.2021.126170>

1118 Shanafield, M., Bourke, S. A., Zimmer, M. A., & Costigan, K. H. (2021). An overview of the
1119 hydrology of non-perennial rivers and streams. *WIREs Water*, 8(2), e1504.

1120 <https://doi.org/10.1002/wat2.1504>

1121 Siskiyou County Water Conservation and Flood Control District. (2021). *Scott Valley*

1122 *Groundwater Sustainability Plan*. Retrieved from

1123 <https://www.co.siskiyou.ca.us/naturalresources/page/scott-valley-final-gsp>

1124 Tolley, D., Foglia, L., & Harter, T. (2019). Sensitivity Analysis and Calibration of an Integrated

1125 Hydrologic Model in an Irrigated Agricultural Basin With a Groundwater-Dependent

1126 Ecosystem. *Water Resources Research*, 55(9), 7876–7901.

1127 <https://doi.org/10.1029/2018WR024209>

1128 Towler, E., Foks, S. S., Dugger, A. L., Dickinson, J. E., Essaid, H. I., Gochis, D., Viger, R. J., &

1129 Zhang, Y. (2023). Benchmarking high-resolution hydrologic model performance of long-

1130 term retrospective streamflow simulations in the contiguous United States. *Hydrology*

1131 *and Earth System Sciences*, 27(9), 1809–1825. [https://doi.org/10.5194/hess-27-1809-](https://doi.org/10.5194/hess-27-1809-2023)

1132 [2023](https://doi.org/10.5194/hess-27-1809-2023)

1133 Trambly, Y., Rutkowska, A., Sauquet, E., Sefton, C., Laaha, G., Osuch, M., Albuquerque, T.,

1134 Alves, M. H., Banasik, K., Beaufort, A., Brocca, L., Camici, S., Csabai, Z., Dakhlaoui,

1135 H., DeGirolamo, A. M., Dörflinger, G., Gallart, F., Gauster, T., ... Datry, T. (2021).

1136 Trends in flow intermittence for European rivers. *Hydrological Sciences Journal*, 66(1),

1137 37–49. <https://doi.org/10.1080/02626667.2020.1849708>

1138 Vázquez-Suñé, E., Abarca, E., Carrera, J., Capino, B., Gámez, D., Pool, M., Simó, T., Batlle, F.,

1139 Niñerola, J. M., & Ibáñez, X. (2006). Groundwater modelling as a tool for the European

1140 Water Framework Directive (WFD) application: The Llobregat case. *Physics and*

1141 *Chemistry of the Earth, Parts A/B/C*, 31(17), 1015–1029.

1142 <https://doi.org/10.1016/j.pce.2006.07.008>

1143 White, J. T., Foster, L. K., & Fienen, M. N. (2021). Extending the Capture Map Concept to

1144 Estimate Discrete and Risk-Based Streamflow Depletion Potential. *Groundwater*, 59(4),

1145 571–580. <https://doi.org/10.1111/gwat.13080>

1146 White, J.T., Hemmings, B., Fienen, M.N. & Knowling, M.J. (2021). Towards improved

1147 environmental modeling outcomes: Enabling low-cost access to high-dimensional,

1148 geostatistical-based decision-support analyses. *Environmental Modelling & Software*,

1149 139, 105022. <https://doi.org/10.1016/j.envsoft.2021.105022>

1150 Winter, T. C., Harvey, J. W., Franke, O. L., & Alley, W. M. (1998). *Ground water and surface*

1151 *water: a single resource*. U.S. Geological Survey.

1152 Zimmerman, J. K. H., Carlisle, D. M., May, J. T., Klausmeyer, K. R., Grantham, T. E., Brown,

1153 L. R., & Howard, J. K. (2018). Patterns and magnitude of flow alteration in California,

1154 USA. *Freshwater Biology*. <https://doi.org/10.1111/fwb.13058>

1155 Zipper, S. C. (2023). streamDepletr: Estimate Streamflow Depletion Due to Groundwater

1156 Pumping (Version R package version 0.2.0). Retrieved from [https://CRAN.R-](https://CRAN.R-project.org/package=streamDepletr)

1157 [project.org/package=streamDepletr](https://CRAN.R-project.org/package=streamDepletr)

1158 Zipper, S. C., Hammond, J. C., Shanafield, M., Zimmer, M., Datry, T., Jones, C. N., Kaiser, K.

1159 E., Godsey, S. E., Burrows, R. M., Blaszcak, J. R., Busch, M. H., Price, A. N., Boersma,

1160 K. S., Ward, A. S., Costigan, K., Allen, G. H., Krabbenhoft, C. A., Dodds, W. K., ...

1161 Allen, D. C. (2021a). Pervasive changes in stream intermittency across the United States.

1162 *Environmental Research Letters*, 16(8), 084033. [https://doi.org/10.1088/1748-](https://doi.org/10.1088/1748-9326/ac14ec)

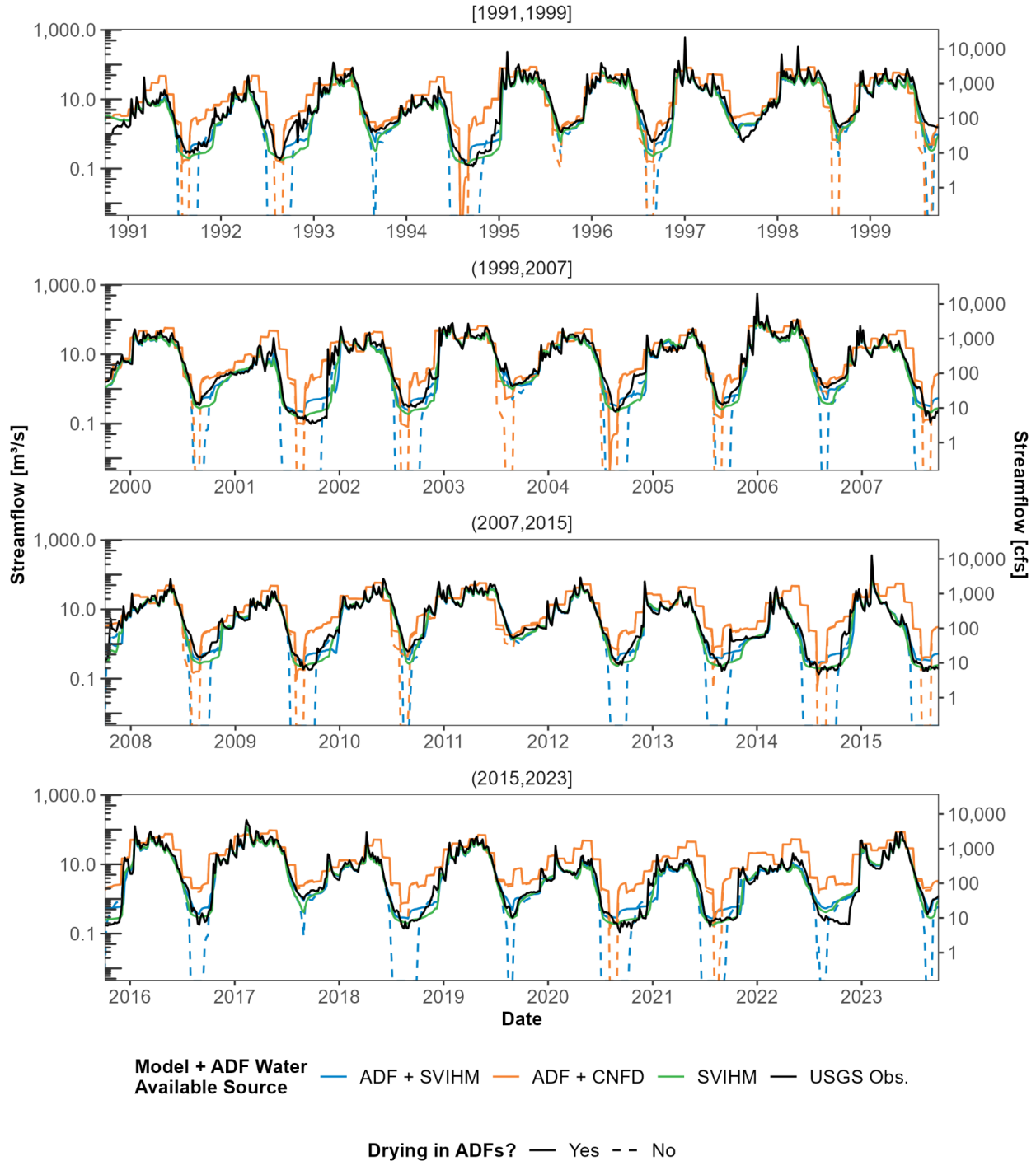
1163 [9326/ac14ec](https://doi.org/10.1088/1748-9326/ac14ec)

1164 Zipper, S. C., Farmer, W. H., Brookfield, A., Ajami, H., Reeves, H. W., Wardropper, C.,

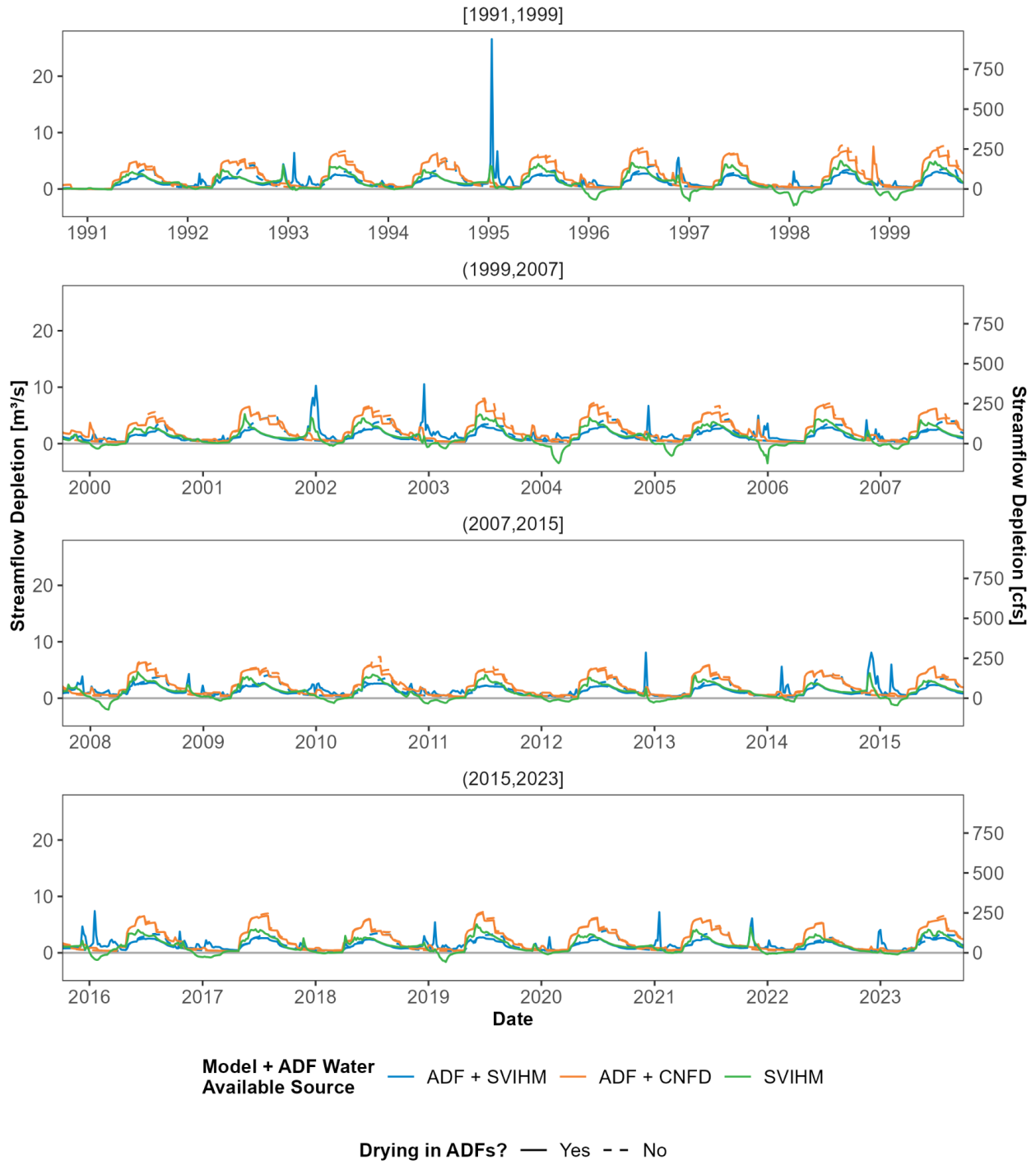
1165 Hammond, J. C., Gleeson, T., & Deines, J. M. (2022a). Quantifying Streamflow

1166 Depletion from Groundwater Pumping: A Practical Review of Past and Emerging
1167 Approaches for Water Management. *JAWRA Journal of the American Water Resources*
1168 *Association*, 58(2), 289–312. <https://doi.org/10.1111/1752-1688.12998>
1169 Zipper, S. C., Dallemagne, T., Gleeson, T., Boerman, T. C., & Hartmann, A. (2018).
1170 Groundwater pumping impacts on real stream networks: Testing the performance of
1171 simple management tools. *Water Resources Research*, 54(8), 5471–5486.
1172 <https://doi.org/10.1029/2018WR022707>
1173 Zipper, S. C., Gleeson, T., Li, Q., & Kerr, B. (2021b). Comparing Streamflow Depletion
1174 Estimation Approaches in a Heavily Stressed, Conjunctively Managed Aquifer. *Water*
1175 *Resources Research*, 57(2), e2020WR027591. <https://doi.org/10.1029/2020WR027591>
1176 Zipper, S. C., Gleeson, T., Kerr, B., Howard, J. K., Rohde, M. M., Carah, J., & Zimmerman, J.
1177 (2019). Rapid and Accurate Estimates of Streamflow Depletion Caused by Groundwater
1178 Pumping Using Analytical Depletion Functions. *Water Resources Research*, 55(7), 5807–
1179 5829. <https://doi.org/10.1029/2018WR024403>
1180 Zipper, S., Kastens, J., Foster, T., Wilson, B.B., Melton, F., Grinstead, A., Deines, J.M., Butler,
1181 J.J. & Marston, L.T. (2024). Estimating irrigation water use from remotely sensed
1182 evapotranspiration data: Accuracy and uncertainties at field, water right, and regional
1183 scales. *Agricultural Water Management*, 303, 109036.
1184 <https://doi.org/10.1016/j.agwat.2024.109036>
1185 Zipper, S., Popescu, I., Compare, K., Zhang, C., & Seybold, E. C. (2022b). Alternative stable
1186 states and hydrological regime shifts in a large intermittent river. *Environmental*
1187 *Research Letters*, 17, 074005. <https://doi.org/10.1088/1748-9326/ac7539>
1188 Zipper, S., Brookfield, A., Ajami, H., Ayers, J. R., Beightel, C., Fienen, M. N., Gleeson, T.,
1189 Hammond, J., Hill, M., Kendall, A. D., Kerr, B., Lapidés, D., Porter, M.,
1190 Parimalarenganayaki, S., Rohde, M. M., & Wardropper, C. (2024). Streamflow Depletion
1191 Caused by Groundwater Pumping: Fundamental Research Priorities for Management-
1192 Relevant Science. *Water Resources Research*, 60(5), e2023WR035727.
1193 <https://doi.org/10.1029/2023WR035727>
1194

1195 Supplemental Information for “Lagged impacts of groundwater pumping on streamflow
 1196 due to stream drying: Incorporation into analytical streamflow depletion estimation
 1197 methods” by Zipper et al.
 1198

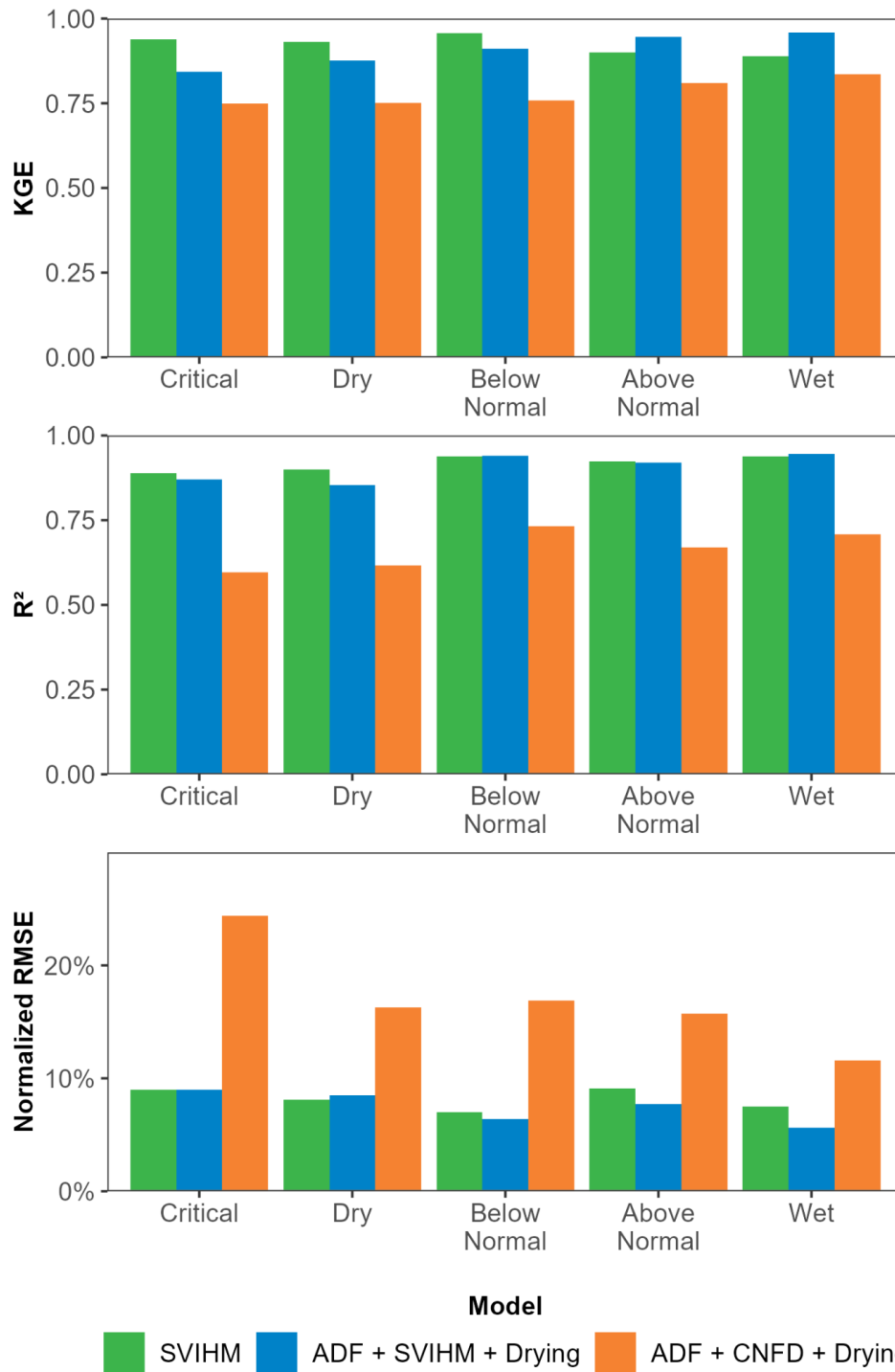


1199
 1200 Figure S1. Streamflow comparison among ADFs, SVIHM, and observations at the watershed outlet for the 33 year
 1201 study period.
 1202



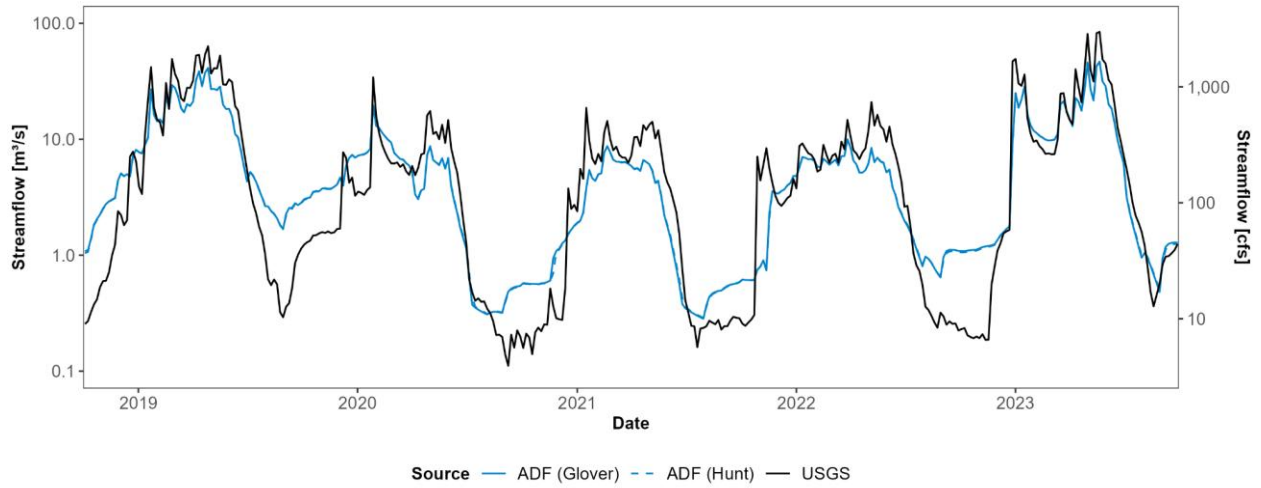
1203
 1204
 1205
 1206

Figure S2. Streamflow depletion comparison between ADFs and SVIHM at the watershed outlet for the 33 year study period.



1207
 1208
 1209
 1210
 1211

Figure S3. Model fit metrics by water year classification. Metrics are calculated via comparison to USGS gauge for log(Streamflow). ADF models include drying. Normalized RMSE is the RMSE divided by the range of observed values.



1212

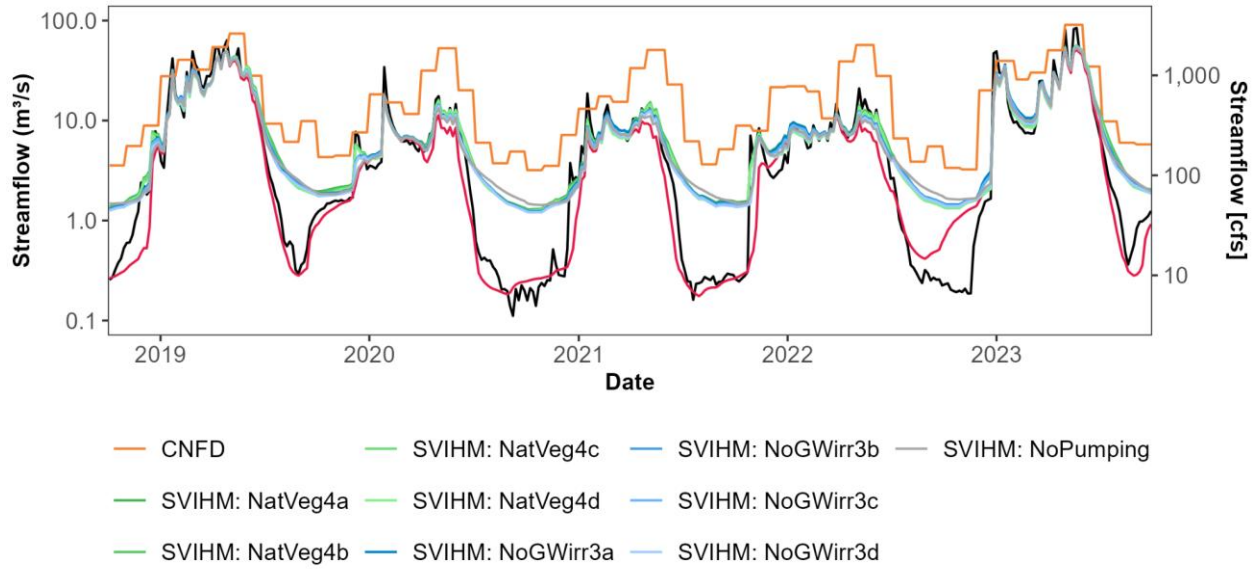
1213 Figure S4. Evaluation of sensitivity of model to choice of analytical solution used in ADFs. The Glover and Hunt
 1214 models produce near-identical results, so the solid and dashed blue lines overlie each other. This indicates that
 1215 streambed conductance is not a limiting factor on streamflow depletion in this domain. All other figures in the
 1216 manuscript use the Hunt model results.

1217

1218 Table S1. Summary of SVIHM model scenarios used in analysis. Scenarios 1 (Basecase) and 3b (No GW Irr Fields)
 1219 are used in the main text.
 1220

ID	Scenario	Land cover or water source changes	SWBM natVeg root depth	natVeg kc for SWBM	natVeg MODFLOW extinction depth	Interpretation of difference from basecase
1	Basecase	Basecase land cover.	Basecase (2.4 m)	Basecase (0.6)	Basecase (0 m; 0.5 m in the Discharge Zone)	N/A
2	No Pumping	Basecase land cover. Water source changes: GW-only → Dry Farming; mixed-GW-SW → SW only				Direct pumping effects, neglecting other land cover-driven changes in water balance. This is not a realistic possibility for real-world, but isolates pumping signal.
3A	No GW-Irrigated Fields	Assign NatVeg land cover to all GW and Mixed-GW-SW fields	1.2m	0.6	3.05 m	Direct pumping effects + difference in water balance due to natural veg replacing ag in GW irrigated fields
3B			2.4m	0.6		
3C			1.2m	1.0		
3D			2.4m	1.0		
4A	Native Vegetation (unimpaired flow)	Assign NatVeg land cover to all cultivated fields	1.2m	0.6		Combined effect of all human modifications
4B			2.4m	0.6		
4C			1.2m	1.0		
4D			2.4m	1.0		

1221



1222

1223

1224

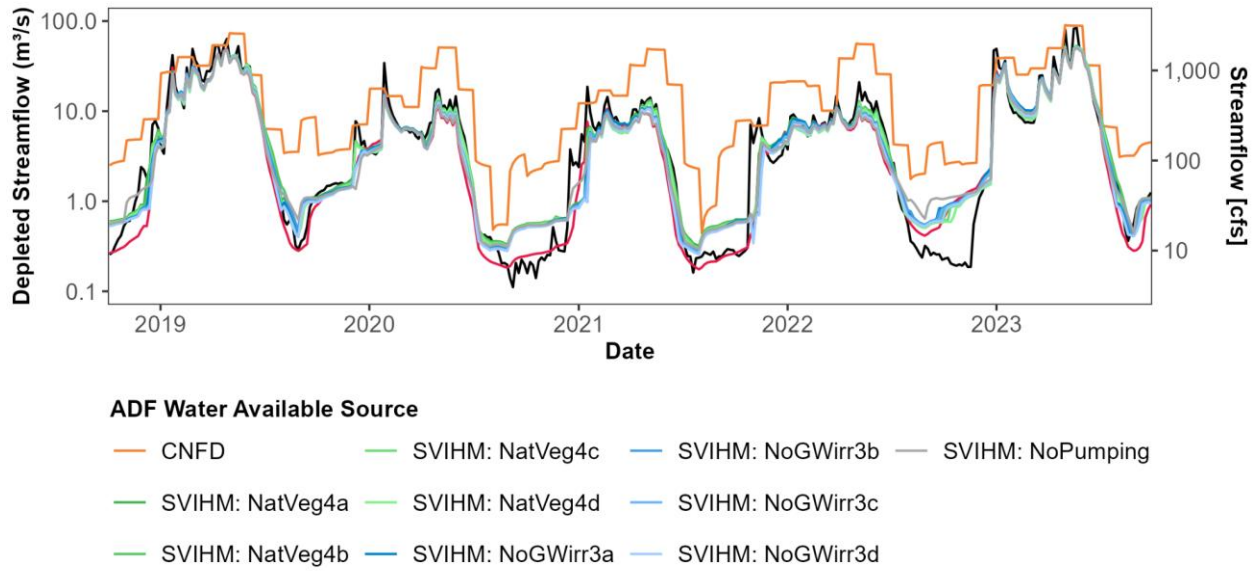
1225

1226

1227

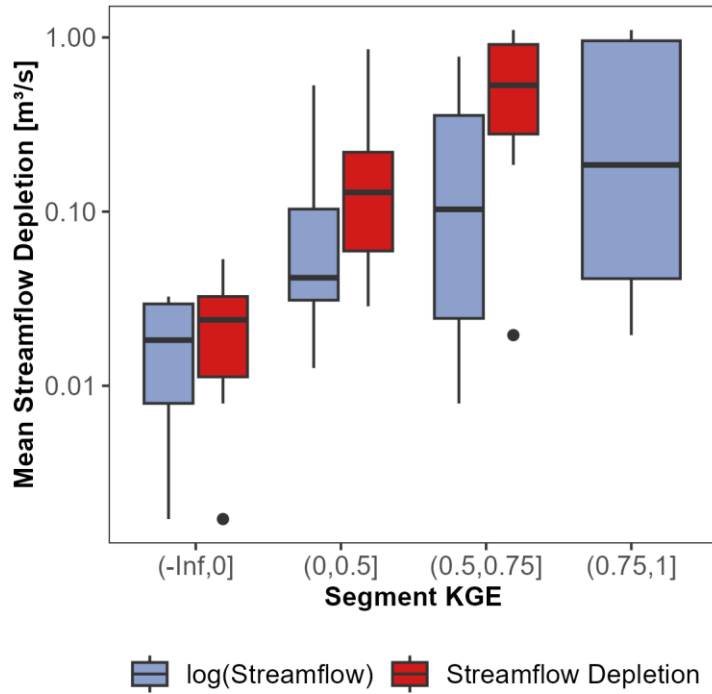
1228

Figure S5. Comparison of streamflow at watershed outlet. The black line shows observed streamflow (source: USGS) and the red line shows the SVIHM basecase (pumped) scenario. The colored lines included in the legend include CNFD unimpaired flows and nine different SVIHM model configurations. The “basecase” (red) and “NoGWirr3b” (blue) scenarios are the basis for results shown in the main text. The other scenarios are meant to show sensitivity to vegetation parameterization, which is described in Table S1.



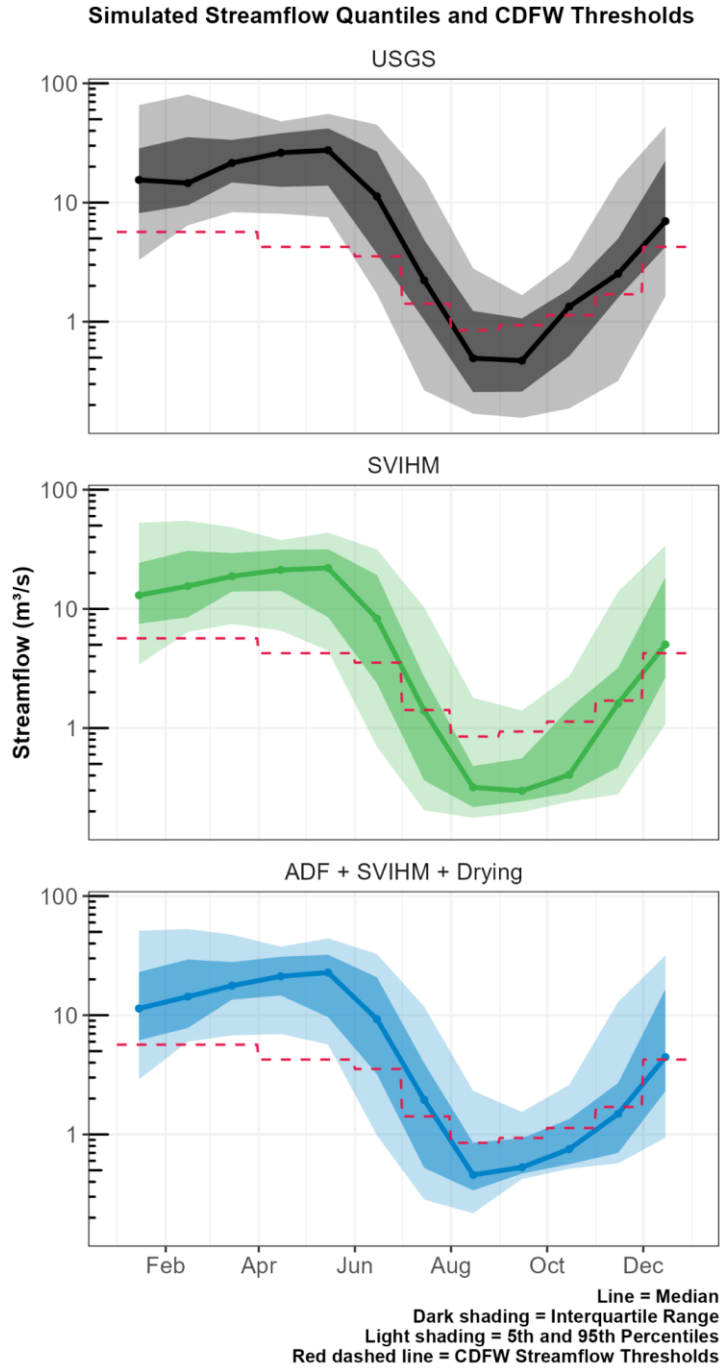
1229
 1230
 1231
 1232
 1233
 1234
 1235
 1236
 1237

Figure S6. Comparison of depleted streamflow at watershed outlet based on ADF simulations using different water available data sources. The black line shows observed streamflow (source: USGS) and the red line shows the SVIHM simulated basecase (pumped) scenario. The colored lines show ADF predicted depleted streamflow using CNFD unimpaired flows and nine different SVIHM model configurations as the water available. ADF models on this plot include drying. The “basecase” (red) and “NoGWirr3b” (blue) scenarios are the basis for results shown in the main text. The other scenarios are meant to show sensitivity to vegetation parameterization, which is described in Table S1.



1238
 1239
 1240
 1241
 1242
 1243

Figure S7. Segment-resolution agreement between ADFs and SVIHM as a function of segment mean streamflow depletion (from SVIHM) in each segment. These results show the ADF + SVIHM + Drying model configuration with water available and SVIHM streamflow depletion calculated using the the SVIHM no-pumping scenario (#2 in Table S1).



1244

1245 Figure S8. Streamflow drought thresholds (red dashed lined) and long-term median, interquartile range, and 5th-95th
 1246 percentile range for streamflow from the USGS observations, SVIHM, and ADF + SVIHM + Drying models.

1247